16 Other Two-Terminal Devices

CHAPTER OBJECTIVES

To become familiar with the characteristics and areas of application of

- Schottky barrier and varactor diodes
- Solar cells, photodiodes, photoconductive cells, and IR emitters
- LCDs
- Thermistors
- Tunnel diodes

16.1 INTRODUCTION

There are a number of two-terminal devices having a single *p–n* junction like the semiconductor or Zener diode but with different modes of operation, terminal characteristics, and areas of application. A number, including the Schottky barrier, varactor, solar cell, photodiode, IR emitter and tunnel diodes, will be introduced in this chapter. In addition, two-terminal devices of a different construction, such as the photoconductive cell, LCD (liquid-crystal display), and thermistor, will be examined.

16.2 SCHOTTKY BARRIER (HOT-CARRIER) DIODES

There has been increasing interest in a two-terminal device referred to as a *Schottky-barrier, surface-barrier,* or *hot-carrier* diode. Its areas of application were first limited to the very high frequency range due to its quick response time (especially important at high frequencies) and lower noise figure (a quantity of real importance in high-frequency applications). In recent years, however, it is appearing more and more in low-voltage/high-current power supplies and ac-to-dc converters. Other areas of application of the device include radar systems, Schottky TTL logic for computers, mixers and detectors in communication equipment, instrumentation, and analog-to-digital converters.

Its construction is quite different from the conventional *p–n* junction in that a metal–semiconductor junction is created such as shown in Fig. 16.1. The semiconductor is normally *n*-type silicon (although *p*-type silicon is sometimes used), whereas a host of different metals, such as molybdenum, platinum, chrome, or tungsten, are used. Different construction techniques result in a different set of characteristics for the device, such as increased frequency range, lower forward bias, and so on. In general, however, Schottky diode construction results in a more uniform junction region and a high level of ruggedness.

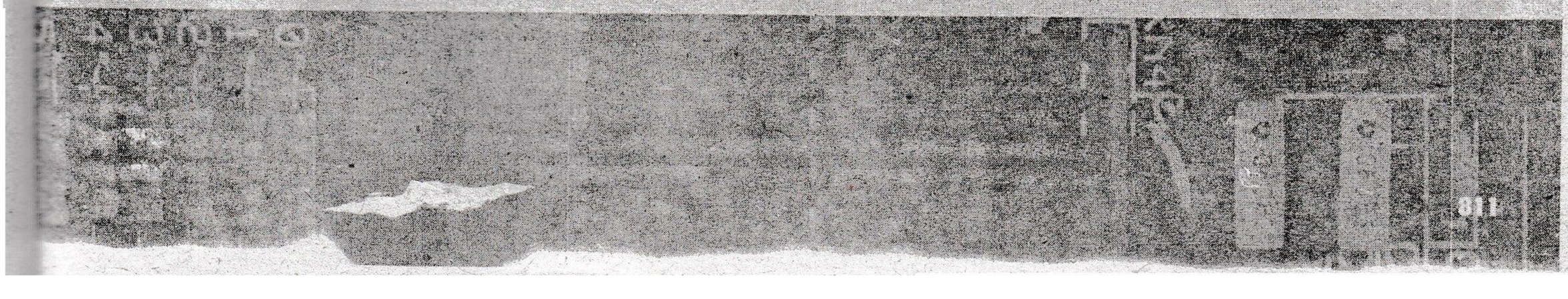

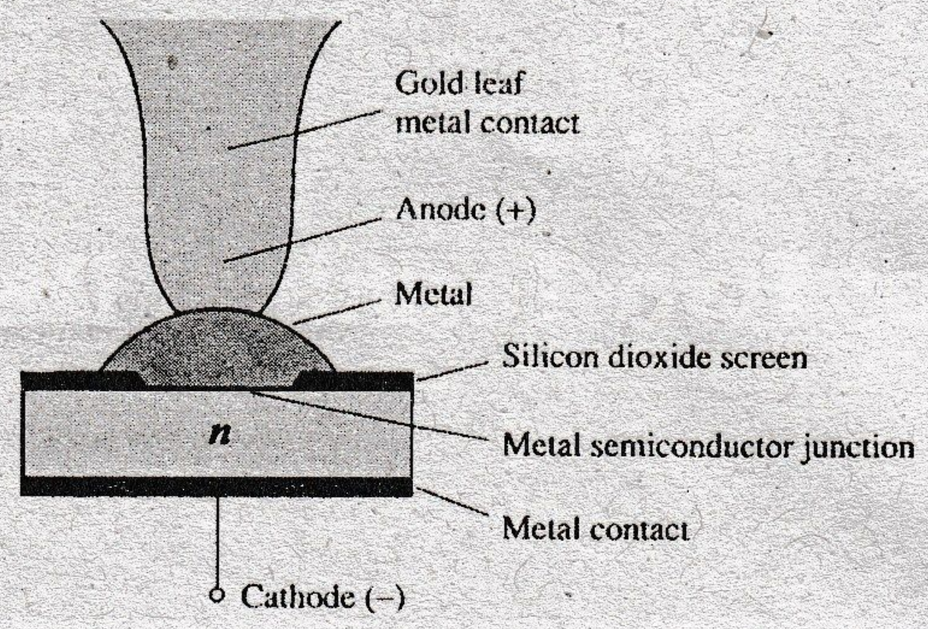

FIG. 16.1
Schottky diode.

In both materials, the electron is the majority carrier. In the metal, the level of minority carriers (holes) is insignificant. When the materials are joined, the electrons in the *n*-type silicon semiconductor material immediately flow into the adjoining metal, establishing a heavy flow of majority carriers. Since the injected carriers have a very high kinetic energy level compared to the electrons of the metal, they are commonly called "hot carriers." In the conventional *p–n* junction, there was the injection of minority carriers into the adjoining region. Here the electrons are injected into a region of the same electron plurality. Schottky diodes are therefore unique in that conduction is entirely by majority carriers. The heavy flow of electrons into the metal creates a region near the junction surface depleted of carriers in the silicon material—much like the depletion region in the *p–n* junction diode. The additional carriers in the metal establish a "negative wall" in the metal at the boundary between the two materials. The net result is a "surface barrier" between the two materials, preventing any further current. That is, any electrons (negatively charged) in the silicon material face a carrier-free region and a "negative wall" at the surface of the metal.

The application of a forward bias as shown in the first quadrant of Fig. 16.2 will reduce the strength of the negative barrier through the attraction of the applied positive potential for electrons from this region. The result is a return to the heavy flow of electrons across the boundary, the magnitude of which is controlled by the level of the applied bias potential. The barrier at the junction for a Schottky diode is less than that of the *p–n* junction device in both the forward- and reverse-bias regions. The result is therefore a higher current at the

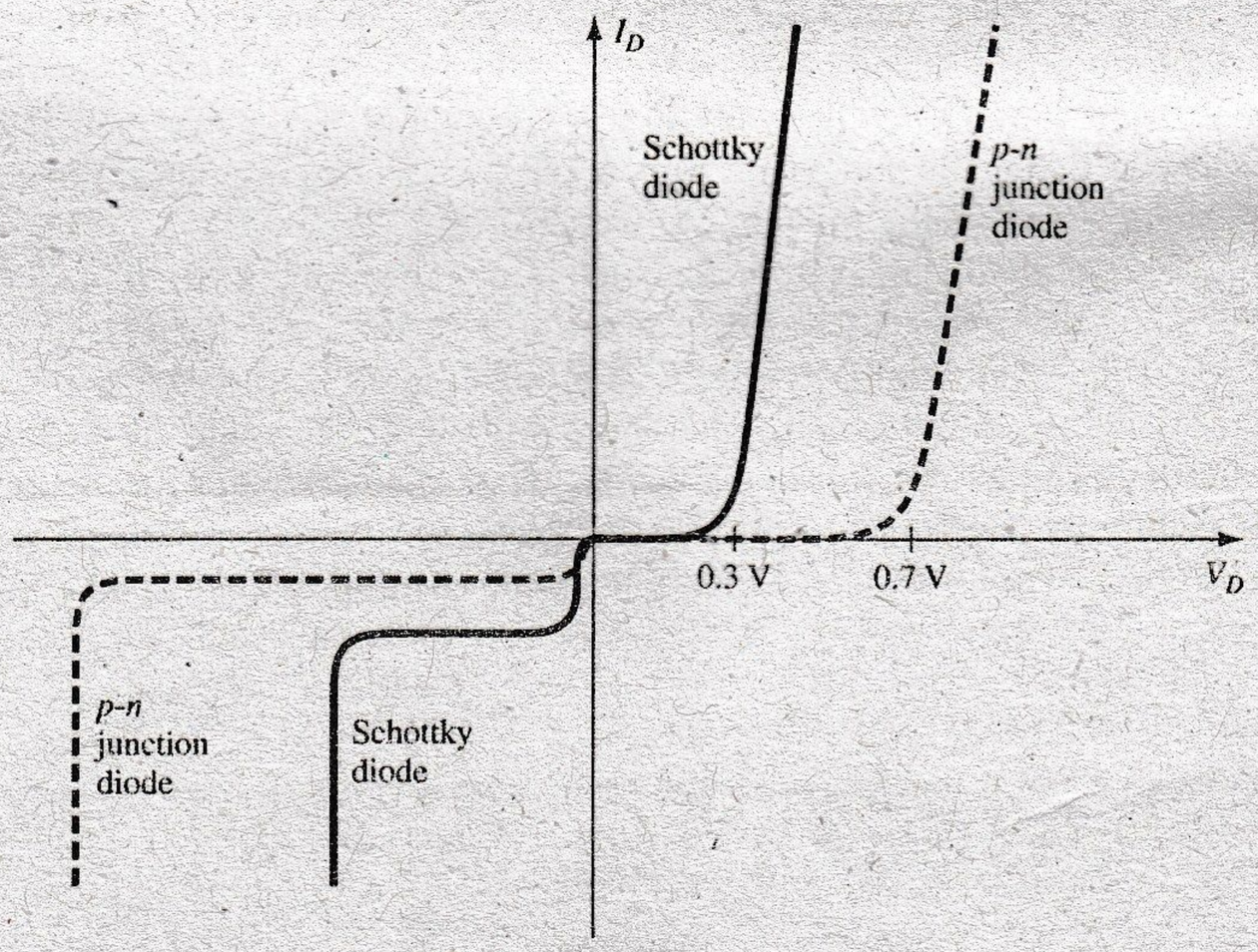

FIG. 16.2
Comparison of characteristics of hot-carrier and p–n junction diodes.

same applied bias in the forward- and reverse-bias regions. This is a desirable effect in the forward-bias region but highly undesirable in the reverse-bias region.

The exponential rise in current with forward bias is described by Eq. (1.2) but with n dependent on the construction technique (1.05 for the metal-whisker type of construction, which is somewhat similar to the germanium diode). In the reverse-bias region, the current I_s is due primarily to those electrons in the metal passing into the semiconductor material. One of the areas of continuing research on the Schottky diode centers on reducing the high leakage currents that result with temperatures over 100°C. Through design, improved units are available that have a temperature range from −65°C to +150°C. At room temperature, I_s is typically in the microampere range for low-power units and the milliampere range for high-power devices, although it is typically larger than that encountered using conventional p–n junction devices with the same current limits. In addition, the PIV of Schottky diodes is usually significantly less than that of a comparable p–n junction unit. Typically, for a 50-A unit, the PIV of the Schottky diode is typically 50 V or less as compared to 150 V for the p–n junction variety. Recent advances, however, have resulted in Schottky diodes with PIVs greater than 100 V at this current level. It is obvious from the characteristics of Fig. 16.2 that the Schottky diode is closer to the ideal set of characteristics than the point contact and has levels of V_T less than those of the typical silicon semiconductor p–n junction. The level of V_T for the "hot-carrier" diode is controlled to a large measure by the metal employed. There is a trade-off between temperature range and level of V_T. An increase in one appears to correspond to a resulting increase in the other. In addition, the lower the range of allowable current levels, the lower is the value of V_T. For some low-level units, the value of V_T can be assumed to be essentially zero on an approximate basis. For the middle and high ranges, however, a value of 0.2 V appears to be a good representative value.

The maximum current rating of Schottky diodes is limited at present to about 100 A. One of the primary areas of application of this diode is in *switching power supplies* that operate in the frequency range of 20 kHz or more. A typical unit at 25°C may be rated at 50 A at a forward voltage of 0.6 V with a recovery time of 10 ns for use in one of these supplies. A p–n junction device with the same current limit of 50 A may have a forward voltage drop of 1.1 V and a recovery time of 30 ns to 50 ns. The difference in forward voltage may not appear significant, but consider the power dissipation difference: $P_{\text{hot carrier}} = (0.6\text{ V})(50\text{ A}) = 30\text{ W}$ compared to $P_{p\,n} = (1.1\text{ V})(50\text{ A}) = 55\text{ W}$, which is a measurable difference when efficiency criteria must be met. There will, of course, be a higher dissipation in the reverse-bias region for the Schottky diode due to the higher leakage current, but the total power loss in the forward- and reverse-bias regions is still significantly improved as compared to the p–n junction device.

Recall from our discussion of reverse recovery time in Chapter 1 that the injected minority carriers accounted for the high level of t_{rr}. The absence of minority carriers at any appreciable level in the Schottky diode results in a reverse recovery time of significantly lower levels, as indicated above. This is the primary reason Schottky diodes are so effective at frequencies approaching 20 GHz, where the device must switch states at a very high rate. For higher frequencies the point-contact diode, with its very small junction area, is still employed.

The equivalent circuit for the device (with typical values) and a commonly used symbol appear in Fig. 16.3. A number of manufacturers prefer to use the standard diode symbol for the device since its function is essentially the same. The inductance L_P and capacitance C_P are package values, and r_B is the series resistance, which includes the contact and the bulk resistance. The resistance r_d and the capacitance C_J are defined by equations introduced in earlier chapters. For many applications, an excellent approximate equivalent circuit simply includes an ideal diode in parallel with the junction capacitance as shown in Fig. 16.4.

A general-purpose Schottky diode manufactured by the Vishay Corporation appears in Fig. 16.5 with the maximum ratings and electrical characteristics. Note in the maximum ratings that the peak V_R is limited to 30 V and the maximum forward current is limited to 200 mA = 0.2 A. However, it can handle a surge current of 5 A if necessary. The electrical characteristics reveal that at low currents neighboring 1 mA (just above the turn-on level) the forward voltage is a maximum of 0.32 V, which is significantly less than the 0.7 V of a typical silicon diode. The current must reach a level approaching 80 mA before the forward

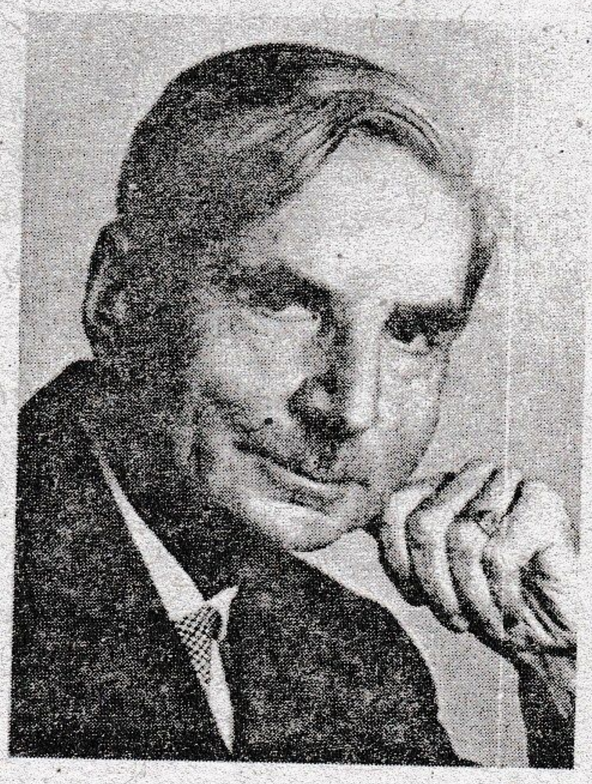

German (Marburg and Berlin, Germany)
(1886–1976)
Professor of Theoretical Physics—University of Rostock
Research Physicist—Siemens Industrial Research Laboratories

Dr. Walter Hermann Schottky was born in Zurich, Switzerland, on July 23, 1886. After obtaining his bachelor of science degree in physics from the University of Berlin in 1908 he obtained his PhD in physics at the university in 1912.

Best known for the Schottky effect, which defines the interaction between a point charge and a flat metal surface. An effect resulting in the popular Schottky diode that has a number of important improvements over the typical semiconductor diode. He is also recognized for the invention of the superhet, the tetrode thermonic valve (multigrid-vacuum tube) and co-invention (with Erwin Gerlach) of the ribbon microphone.

Awards include the Royal Society Hughes award in 1936 and the Werner-von-Siemens-Ring in 1964. In addition the Walter Schottky Institute in Germany is named after him.

Dr. Walter Herman Schottky
(Photo courtesy of the Siemens Corporate Archives, Munich.)

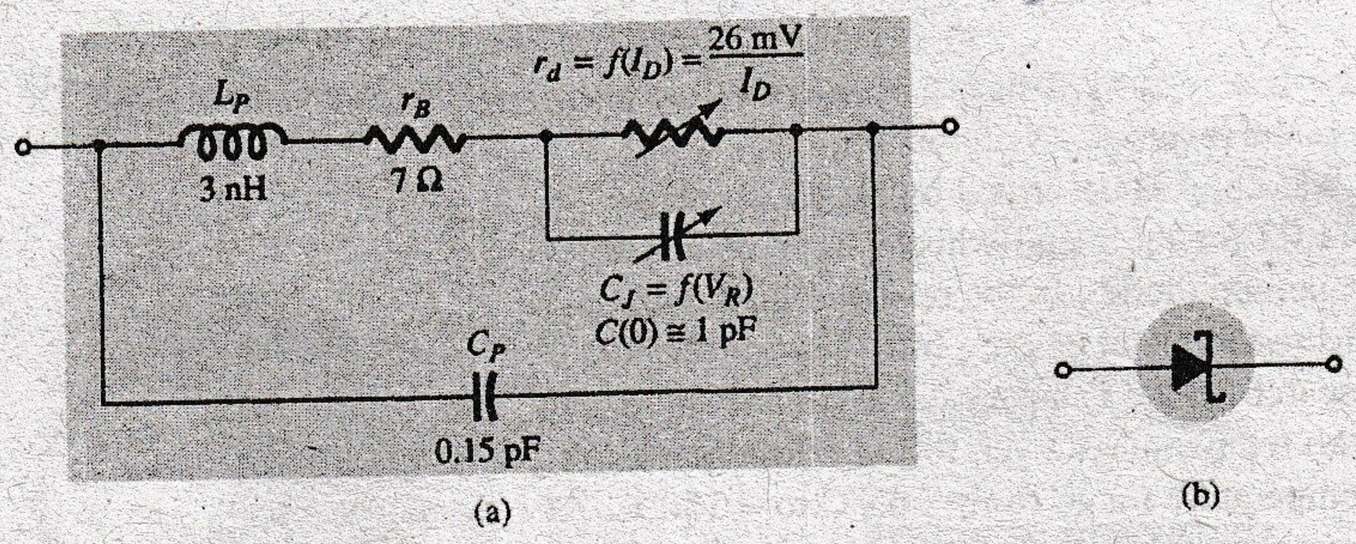

FIG. 16.3
Schottky (hot-carrier) diode: (a) equivalent circuit; (b) symbol.

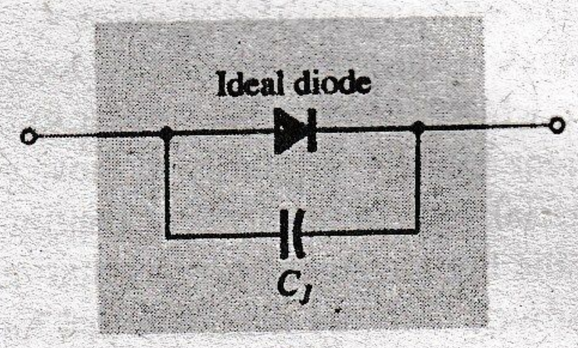

FIG. 16.4
Approximate equivalent circuit for the Schottky diode.

Small-Signal Schottky Diode

Applications
- Applications where a very low forward voltage is required

ABSOLUTE MAXIMUM RATINGS T_{amb} = 25°C, unless otherwise specified

Parameter	Test Condition	Symbol	Value	Unit
Reverse voltage		V_R	30	V
Peak forward surge current	t_p = 10 ms	I_{FSM}	5	A
Repetitive peak forward current	$t_p \leq 1$ s	I_{FRM}	300	mA
Forward current		I_F	200	mA
Average forward current		I_{FAV}	200	mA

THERMAL CHARACTERISTICS T_{amb} = 25°C, unless otherwise specified

Parameter	Test Condition	Symbol	Value	Unit
Junction to ambient air	on PC board 50 mm × 50 mm × 1.6 mm	R_{thJA}	320	K/W
Junction temperature		T_j	125	°C
Storage temperature range		T_{stg}	–65 to + 150	°C

ELECTRICAL CHARACTERISTICS T_{amb} = 25°C, unless otherwise specified

Parameter	Test Condition	Symbol	Min	Typ.	Max	Unit
Forward voltage	I_F = 0.1 mA	V_F			240	mV
	I_F = 1 mA	V_F			320	mV
	I_F = 10 mA	V_F			400	mV
	I_F = 30 mA	V_F			500	mV
	I_F = 100 mA	V_F			800	mV
Reverse current	V_R = 25 V, t_p = 300 µs	I_R			2.3	µA
Diode capacitance	V_R = 1 V, f = 1 MHz	C_D			10	pF

FIG. 16.5
Maximum ratings, thermal characteristics, and electrical characteristics for a Vishay BAS285 Schottky diode.

voltage reaches a level that approaches 0.7 V. For switching applications the capacitance level is important, but the level of 10 pF is generally acceptable for most applications. Finally, note that the reverse current is only 2.3 μA.

The typical characteristics of the device appear in Fig. 16.6. In Fig. 16.6a we find that the forward voltage is about 0.5 V at 20 mA but drops to about 0.45 V at 10 mA. At 0.1 mA

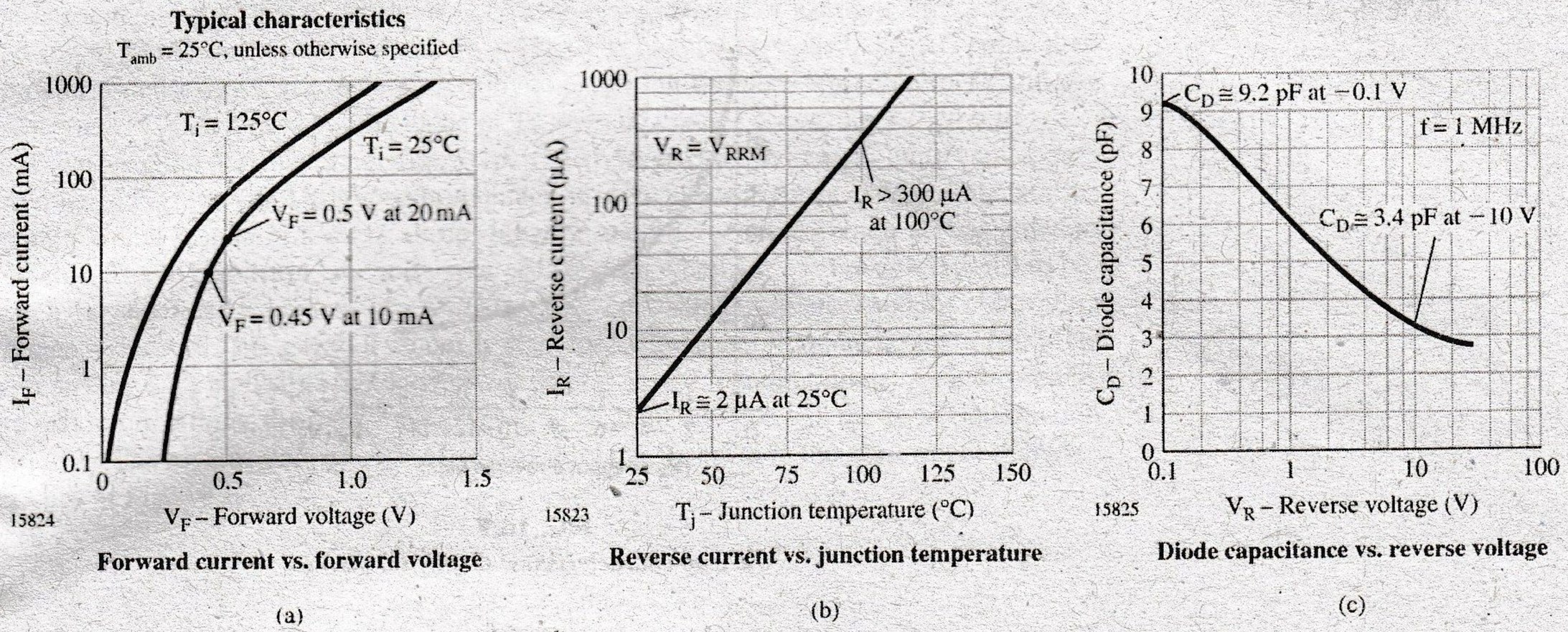

FIG. 16.6

Typical characteristics for a Vishay BAS285 Shottky diode.

the forward voltage drops to only 0.25 V. In Fig. 16.6b we find that the reverse current increases rapidly with temperature. At 100°C it is exceeding 300 μA = 0.3 mA, which is quite excessive. Fortunately at lower temperatures such as 25°C it is only 2 μA. Fig. 16.6c reveals why the capacitive element is an integral part of the equivalent circuit. At $V_R = -0.1$ V it is close to 9.2 pF, whereas at $V_R = -10$ V it has dropped to 3.4 pF.

16.3 VARACTOR (VARICAP) DIODES

Varactor (also called varicap, VVC [voltage-variable capacitance], or tuning) diodes are semiconductor, voltage-dependent, variable capacitors. Their mode of operation depends on the capacitance that exists at the p–n junction when the element is reverse-biased. Under reverse-bias conditions, there is a region of uncovered charge on either side of the junction that together make up the depletion region and define the depletion width W_d. The transition capacitance C_T established by the isolated uncovered charges is determined by

$$C_T = \epsilon \frac{A}{W_d} \tag{16.1}$$

where ϵ is the permittivity of the semiconductor materials, A is the p–n junction area, and W_d is the depletion width.

As the reverse-bias potential increases, the width of the depletion region increases, which in turn reduces the transition capacitance: The characteristics of a typical commercially available varicap diode appear in Fig. 16.7. Note the initial sharp decline in C_T with increase in reverse bias. The normal range of V_R for VVC diodes is limited to about 20 V. In terms of the applied reverse bias, the transition capacitance is given approximately by

$$C_T = \frac{K}{(V_T + V_R)^n} \tag{16.2}$$

where K = constant determined by the semiconductor material and construction technique
V_T = knee potential as defined in Section 1.6
V_R = magnitude of the applied reverse-bias potential
$n = \frac{1}{2}$ for alloy junctions and $\frac{1}{3}$ for diffused junctions

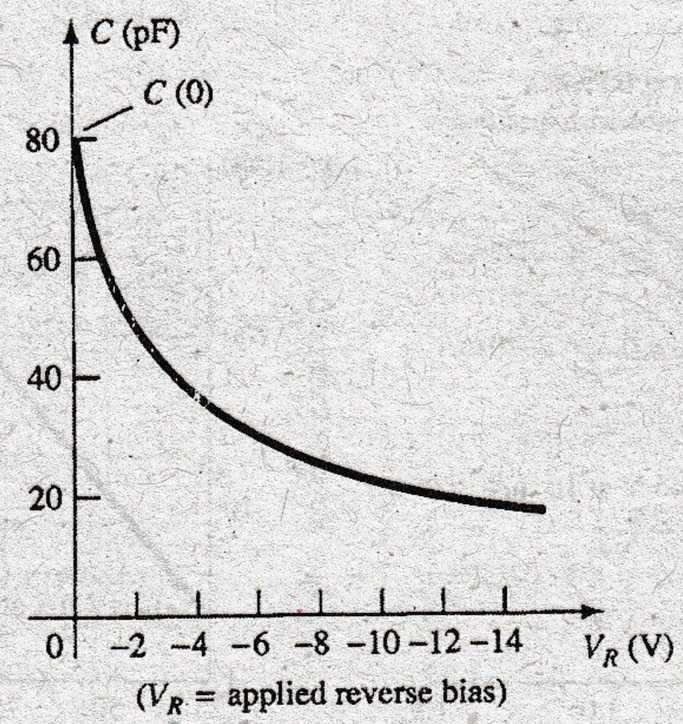

FIG. 16.7
Varicap characteristics: C (pF) versus V_R.

In terms of the capacitance at the zero-bias condition $C(0)$, the capacitance as a function of V_R is given by

$$C_T(V_R) = \frac{C(0)}{\left(1 + |V_R/V_T|\right)^n} \tag{16.3}$$

The symbols most commonly used for the varicap diode and a first approximation for its equivalent circuit in the reverse-bias region are shown in Fig. 16.8. Since we are in the reverse-bias region, the resistance in the equivalent circuit is very large in magnitude—typically 1 MΩ or larger—whereas R_S, the geometric resistance of the diode, is, as indicated in Fig. 16.8, very small. The magnitude of C_T will vary from about 2 pF to 100 pF depending on the varicap considered. To ensure that R_R is as large (for minimum leakage current) as possible, silicon is normally used in varicap diodes. The fact that the device will be employed at very high frequencies requires that we include the inductance L_S even though it is measured in nanohenries. Recall that $X_L = 2\pi fL$, and a frequency of 10 GHz with $L_S = 1$ nH results in $X_{L_S} = 2\pi fL = (6.28)(10^{10}\,\text{Hz})(10^{-9}\,\text{F}) = 62.8\,\Omega$. There is obviously, therefore, a frequency limit associated with the use of each varicap diode. Assuming the proper frequency range and a low value of R_S and X_{L_S} compared to the other series elements, then we can replace the equivalent circuit for the varicap of Fig. 16.8a by the variable capacitor alone.

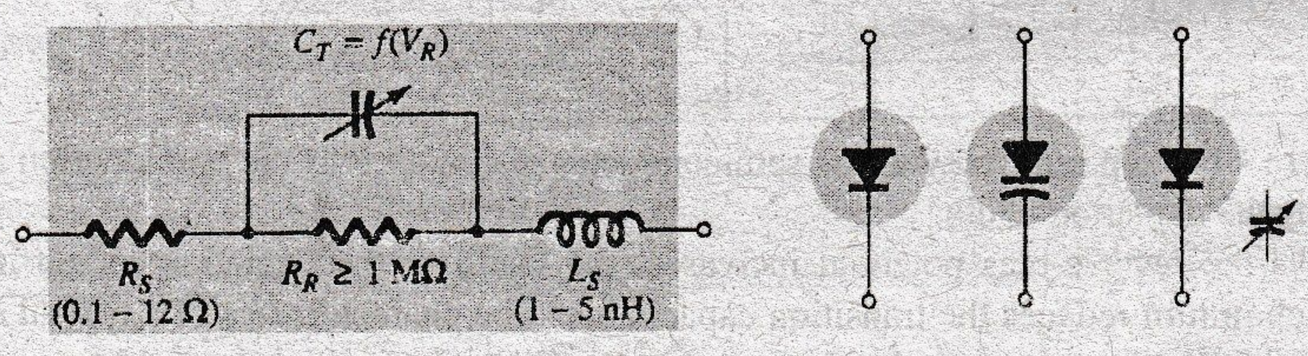

FIG. 16.8
Varicap diode: (a) equivalent circuit in the reverse-bias region; (b) symbols.

The *capacitance temperature coefficient* is defined by

$$TC_C = \frac{\Delta C}{C_0(T_1 - T_0)} \times 100\% \quad \%/^\circ\text{C} \tag{16.4}$$

where ΔC is the change in capacitance due to the temperature change $T_1 - T_0$ and C_0 is the capacitance at T_0 for a particular reverse-bias potential. For example, at $V_R = -3$ V and $C_0 = 29$ pF with $V_R = 3$ V and $T_0 = 25°C$. A change in capacitance ΔC could then be determined using Eq. (16.4) simply by substituting the new temperature T_1 and the associated TC_C. At a new V_R, the value of TC_C would change accordingly.

The packaging and maximum ratings for a Micrometrics hyperabrupt tuning varactor are provided in Fig. 16.9(a). The hyperabrupt junction is created using a special ion-implantation technique that results in a more abrupt junction than the more common abrupt junction varactor. The hyperabrupt junction varactor is chosen when a more linear relationship between the generated frequency of a VCO (voltage-controlled oscillator) and the controlling voltage is desired. This series of diodes is ideal for LC resonant frequencies up to 100 MHz with an almost straight-line relationship for the 1.5 V to 4 V tuning range. As indicated by the maximum ratings, the peak forward current is about 100 mA and the power dissipation 250 mW. The reverse voltage rating is defined by the V_{br} level in the performance characteristics of Fig. 16.10.

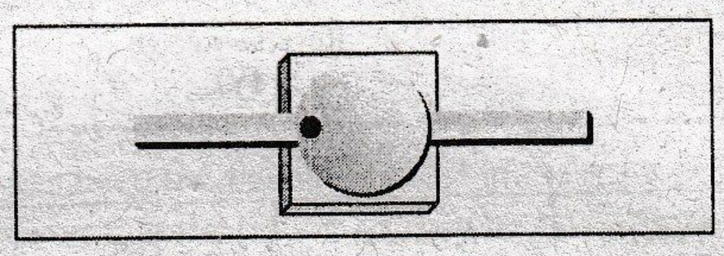

(a)

Maximum Ratings

Parameter	Symbol	Value	Units
Reverse voltage	V_r	Same as V_{br}	Volts
Forward current	I_f	100	mA
Power dissipation	Pd (25°C)	250	mW
Operating temperature	T_{op}	−55 to +150	°C
Storage temperature	T_{stg}	−65 to +200	°C

(b)

FIG. 16.9

Micrometrics hyperabrupt tuning varactor: (a) packaging; (b) maximum ratings.

The electrical characteristics and typical performance characteristics are provided in Fig. 16.10. Note for the TV 1401 that the capacitance can run from about 58 pF at a reverse voltage of 2 V down to 6.1 pF at a reverse voltage of 7 V validating the drop-off curve of Fig. 16.7. It then continues to drop to about 5 pF at a reverse voltage of 10 V. For varactor diodes the tuning ratio is important in the sense that it gives a quick idea of how much the capacitance will change between typical operating ranges of applied voltage. As shown in the electrical characteristics the capacitance will typically drop by a factor of 13 when the reverse voltage is changed from 1.25 V to 7 V. For the change from 2 V to 10 V the change in capacitance is in the range of 10 to 17, depending on the unit. The change in capacitance is plotted in Fig. 16.10(a) for the full range of anticipated application. For the range of reverse voltage shown, the capacitance drops from about 130 pF (log scale) at $V_r = 0.1$ V to about 4 pF $V_r = 15$ V. The quality factor Q is defined as introduced for resonant circuits in earlier sections of this text. It is an important factor when the varactor is used in oscillator design because it can have a pronounced effect on the noise performance level. A high Q will result in a high-selectivity response curve and a rejection of frequencies associated with noise. At a reverse voltage of 2 V and a typical operating frequency of 10 MHz the Q factor is quite high at a typical level of 140 and minimum level of 75. Note the provided curve for Q versus reverse voltage for a fixed frequency of 10 MHz. It increases rapidly with reverse voltage because the total junction capacitance drops with reverse voltage.

Typical Performance

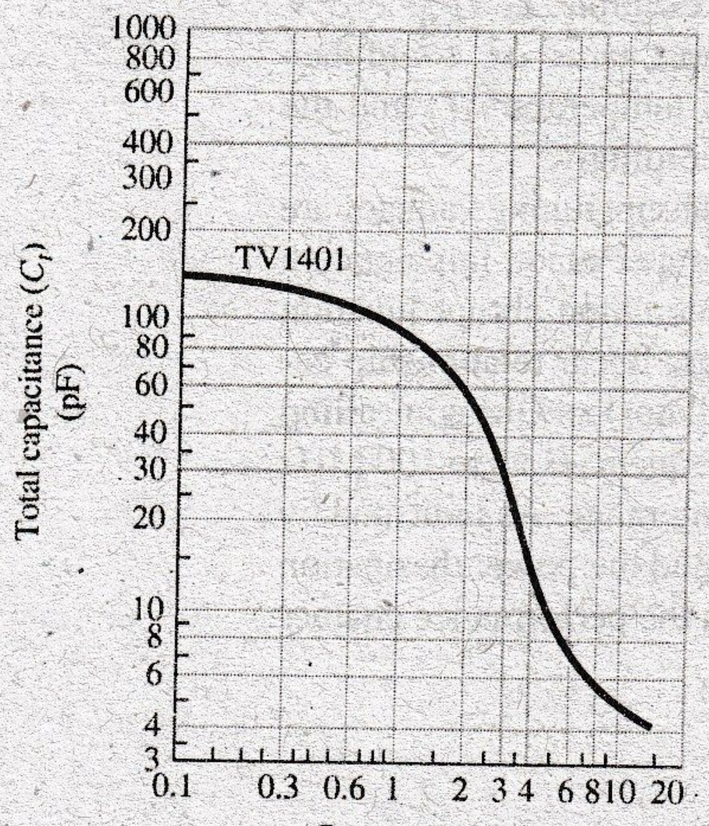

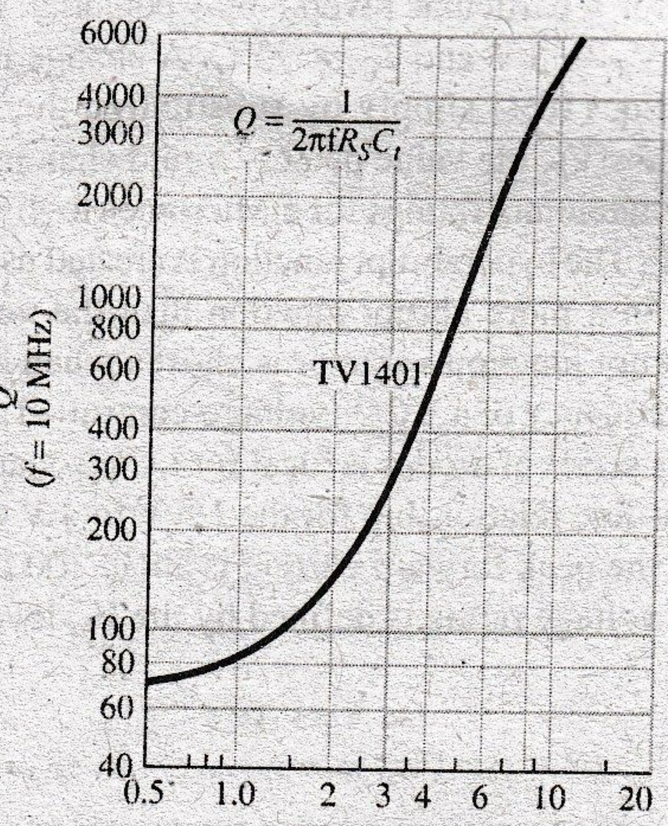

Q V_r = 2 Vdc		V_{br} (Vdc) I_r = 10 μ Adc	I_r (nAdc) V_r = 10 Vdc	Part number
F = 1 MHz MIN/TYP	F = 10 MHz MIN/TYP	MIN/TYP	TYP/MAX	
–	75/140	12/20	10/50	TV1401
200/700	–	12/20	50/100	TV1402
200/700	–	12/20	100/1000	TV1403

(a)

Electrical Characteristics

Total capacitance, C_t F = 1 MHz (pF)				Tuning ratio, T_r F = 1 MHz		Part number
V_r = 2 Vdc MIN/TYP/MAX	V_r = 7 Vdc TYP	V_r = 10 Vdc MIN/TYP/MAX	V_r = 125 Vdc TYP	C(1.25V)/C(7V) TYP	C(2V)/C(10V) MIN/TYP/MAX	
46/57/68	6.1	4.2/4.7/5.2	81.5	13	10/12/17	TV1401
46/57/68	6.1	4.2/4.7/5.2	81.5	13	10/12/17	TV1402
46/57/-	6.1	-/4.7/5.2	81.5	13	10/12/-	TV1403

(b)

FIG. 16.10
Micrometrics TV 1400 series of varactor diodes: (a) typical performance; (b) electrical characteristics.

Some of the high-frequency (as defined by the small capacitance levels) areas of application include FM modulators, automatic-frequency-control devices, adjustable bandpass filters, and parametric amplifiers.

Application

In Fig. 16.11, the varactor diode is employed in a tuning network. That is, the resonant frequency of the parallel LC combination is determined by $f_p = 1/2\pi\sqrt{L_2C_T'}$ (high-Q system) with the level of $C_T' = C_T + C_C$ determined by the applied reverse-bias potential V_{DD}. The coupling capacitor C_C is present to provide isolation between the shorting effect of L_2 and the applied bias. The selected frequencies of the tuned network are then passed on to the high-input amplifier for further amplification.

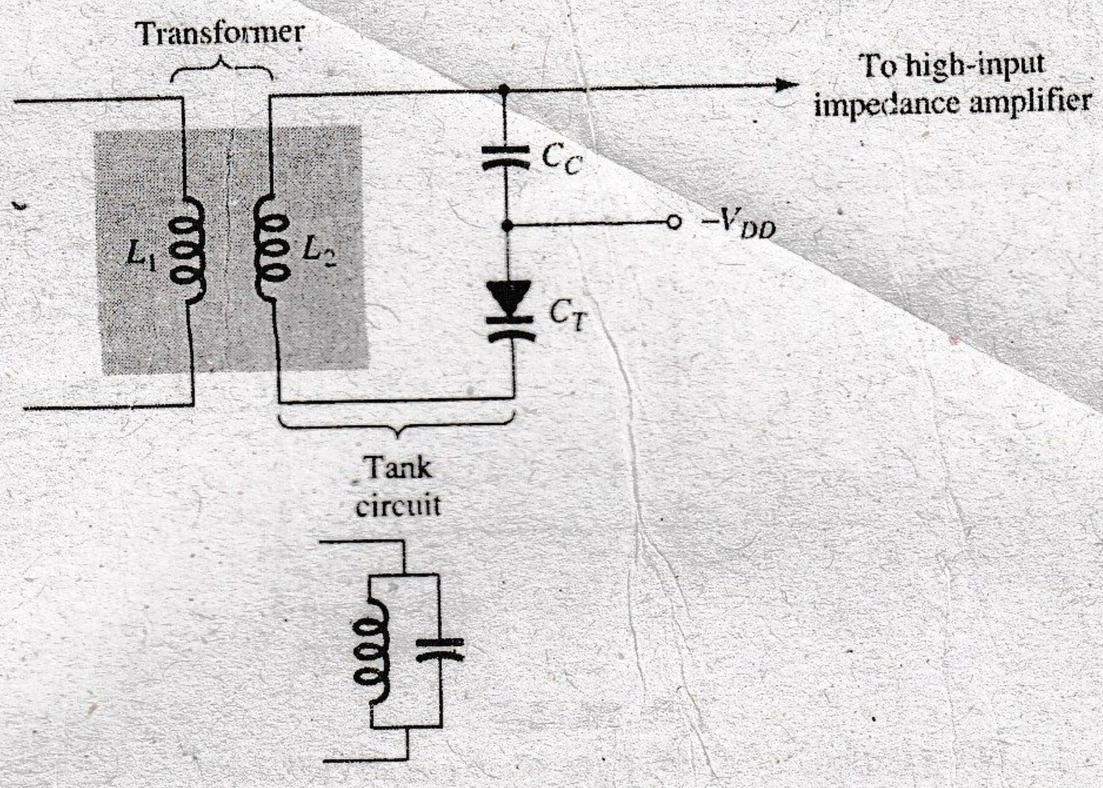

FIG. 16.11
Tuning network employing a varactor diode.

16.4 SOLAR CELLS

In recent years, there has been increasing interest in the solar cell as an alternative source of energy. When we consider that the power density received from the sun at sea level is about 100 mW/cm^2 (1 kW/m^2), it is certainly an energy source that requires further research and development to maximize the conversion efficiency from solar to electrical energy.

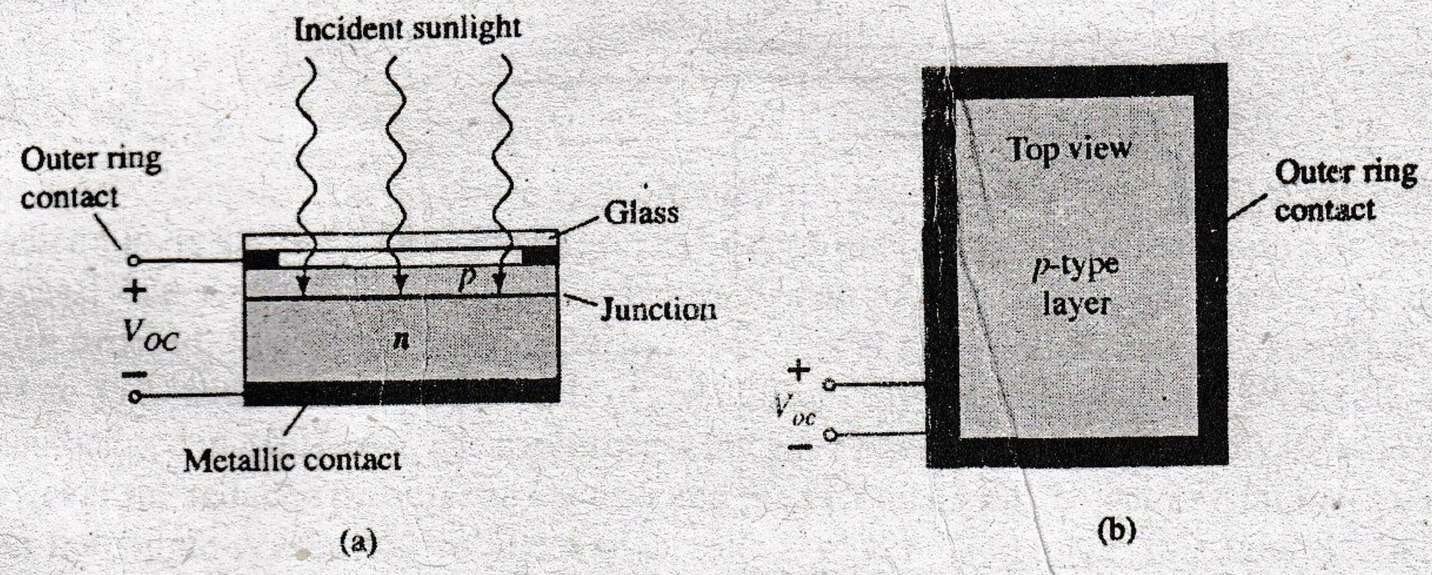

FIG. 16.12
Solar cell: (a) cross section; (b) top view.

The basic construction of a silicon p–n junction solar cell appears in Fig. 16.12. As shown in the top view, every effort is made to ensure that the surface area perpendicular to the sun is a maximum. Also note that the metallic conductor connected to the p-type material and the thickness of the p-type material are such that they ensure that a maximum number of photons of light energy will reach the junction. A photon of light energy in this region may collide with a valence electron and impart to it sufficient energy to leave the parent atom. The result is a generation of free electrons and holes. This phenomenon will occur on each side of the junction. In the p-type material, the newly generated electrons are minority carriers and will move rather freely across the junction as explained for the basic p–n junction with no applied bias. A similar discussion is true for theholes generated in the n-type material. The result is an increase in the minority-carrier flow, which is opposite in direction to the conventional forward current of a p–n junction. The current for a single-cell silicon solar cell will increase in an almost linear fashion with the intensity of the incident light as shown in Fig. 16.13 . Double the incident light will double the resulting current and so on. The plot is for the maximum current generated for a particular level of incident light. Since maximum condition s result when the output is short-circuited as shown in Fig. 16.13, the label for the resulting current is I_{SC}. Under short-circuit conditions the output voltage is 0 V as shown in the same figure.

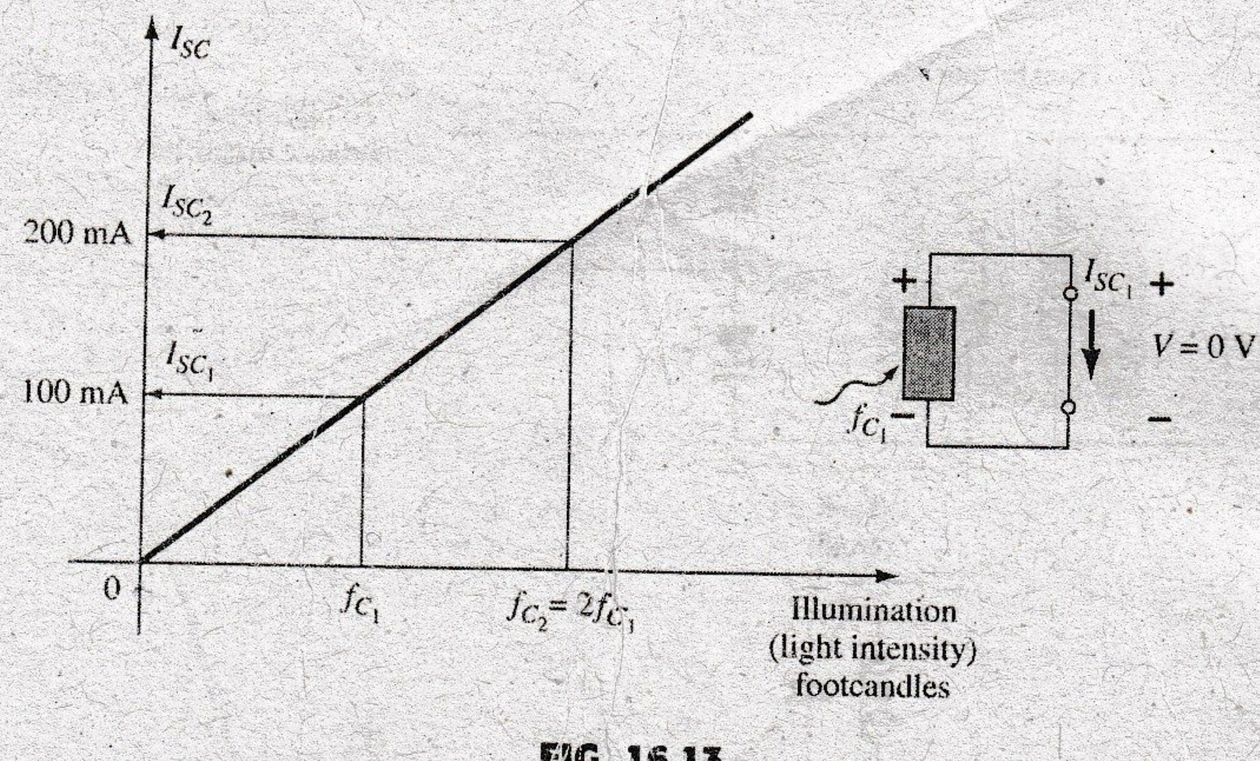

FIG. 16.13
Effect of light intensity on the short-circuit current.

A plot of the open-circuit voltage for the same levels of incident light is provided in Fig. 16.14. Note that it increases very rapidly to a level that stays within the boundaries of 0.5 V to 0.6 V. That is, for the broad range of incident light in Fig. 16.14, the terminal voltage is fairly constant. Since the output voltage is the open-circuit voltage as shown in the same figure, the label for the resulting voltage at each level of incident light is V_{OC}.

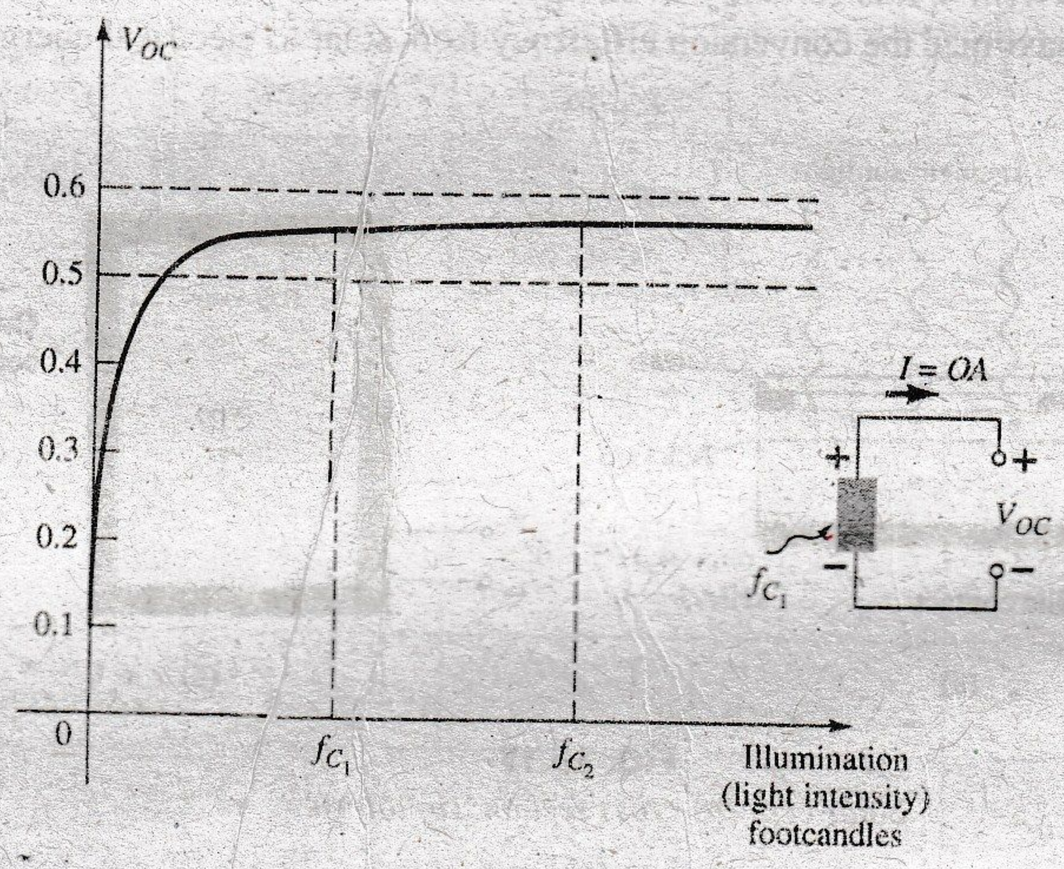

FIG. 16.14
Effect of light intensity on the open-circuit voltage.

In general, therefore,

The open-circuit potential generated by a solar cell is fairly constant, while the short-circuit maximum current will increase in a linear fashion.

Since the voltage is fairly constant, higher output voltages can be established by connecting the solar cells in a series. The current generated in a series configuration will be the same as generated by a single cell. For increased current levels at a single cell open-circuit voltage, solar cells can be connected in parallel.

If a plot of current versus voltage is generated as shown in Fig. 16.15 for a particular incident light, a curve for the power associated with the solar cell can be generated by simply using the equation $P = VI$.

Note in Fig. 16.15 that the short-circuit current is the maximum current with the level of current decreasing with increasing terminal voltage. Also take note that the level of voltage is fairly constant for the range of current from 0 A to just short of the maximum power point. Since the current curve is fairly level for the lower voltage levels, the increase in power is

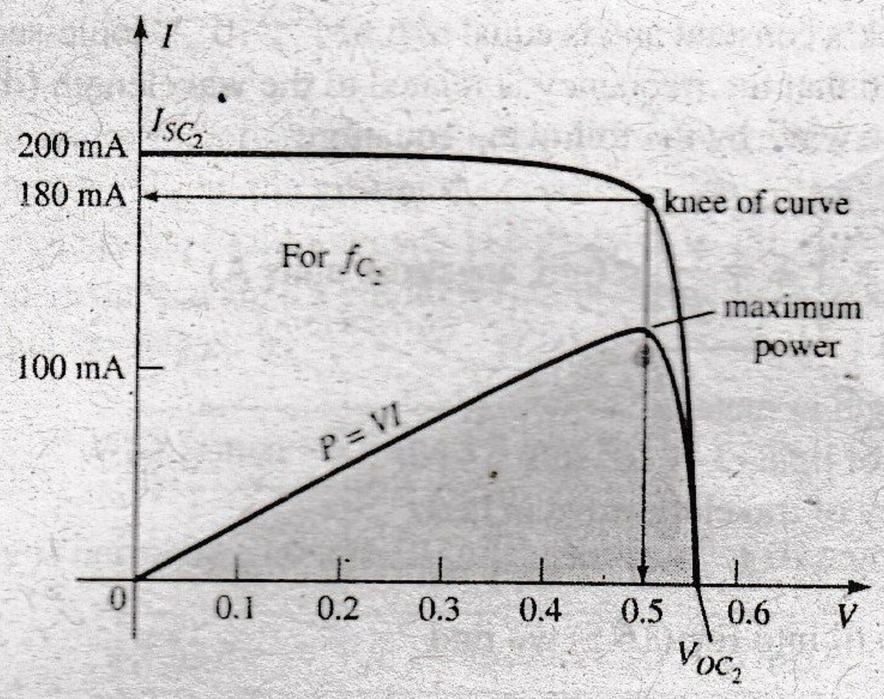

FIG. 16.15
Sketching the power curve for the light intensity f_{C_2}.

due primarily to the increasing levels of voltage using the power equation $P = VI$. Eventually, however, even though the voltage continues to increase, the current drops dramatically near V_{OC} and the power curve drops accordingly. The maximum power occurs in the knee region of the I–V curve as shown in Fig. 16.15. For this cell at f_{C_2} it is approximately

$$P = VI = (0.5\text{ V})(180\text{ mA}) = \mathbf{90\text{ mW}}$$

The level of current that results in a solar cell is directly related to the absorption characteristics of the material (referred to as the absorption coefficient), the wavelength of the incident light, and the intensity of the incident light.

Materials

The most common material in use today in the full range of bulk and thin-film solar cells is silicon in its various forms. Each form to be described is manufactured using a different process. The **single-crystal** silicon structure has an atomic lattice that is uniform, perfectly ordered, and of the highest purity. The typical range of efficiency extends from 14% to 17% with experimental levels of over 20%. **Polycrystalline** silicon solar cells are manufactured in a different, cheaper process but have lower levels of efficiency (9%–14%). However the reduced manufacturing cost and the fact that it can be cut into thinner layers than the single-crystal lattice make such cells a viable alternative. In recent years the introduction of **thin-film** technology has had a broad impact on the cost and range of application of solar cells. The very thin (less than 1 μm in many cases) semiconductor layers are deposited (using various spraying techniques) on a supporting structure such as glass, plastic, or metal. A compound, **amorphous silicon (a-Si),** is currently the most extensively used thin-film material. The reduced production costs, along with the high light absorption characteristics, balance out the efficiency levels that are reduced to single digits (6%–9%).

Another single-crystal compound, **gallium arsenide** (GaAs), is commonly used in bulk solar cells because of its high rate of absorption and higher energy conversion rate in the range 20%–30%. Additional thin-film materials include **cadmium telluride** (CdTe) and **copper indium diseelenide** ($CuInSe_2$ or CIS). CdTe has a very high light absorption level and is less expensive to manufacture with the same conversion efficiency as silicon. CIS is used in leading-edge research with conversion levels approaching 18% with high absorption and conversion rates.

Wavelength

The energy associated with each photon is directly related to the frequency of the traveling wave and determined by the following equation:

$$\boxed{W = Kf} \quad \text{(joules)} \qquad \textbf{(16.5)}$$

where $\mathcal{H}$ is called Planck's constant and is equal to 6.624×10^{-34} joule-seconds. You may recall from Section 1.16 that the frequency is related to the wavelength (distance between successive peaks) of the wave by the following equation:

$$\boxed{\lambda = \frac{v}{f}} \quad \text{(nm, angstrom units Å)} \tag{16.6}$$

where λ = wavelength in meters
v = velocity of light, 3×10^8 m/s
f = frequency of traveling wave in hertz
and $\text{Å} = 10^{-10}$ m, 1 nm $= 10^{-9}$ m

Substituting Eq. (16.6) into Eq. (16.5) we find

$$\boxed{W = \frac{\mathcal{H}v}{\lambda}} \quad \text{(joules)} \tag{16.7}$$

and find that the energy associated with a discrete package of photons is inversely proportional to the wavelength.

Clearly, therefore

The energy associated with the photons being absorbed by the semiconductor layer of a solar cell is a function of the wavelength of the incident light, and the longer the wavelength, the less the associated energy levels.

In addition it is important to realize that

Each photon can only cause the generation of one electron-hole pair. Any photon with energy levels higher than that required to release an electron will simply contribute to the heating of the solar cell.

For silicon, the absorption curve is provided as Fig. 16.16, showing that it peaks around 850 nm. As noted above, since the wavelength is shorter, the energy level associated with the color blue of the visible spectrum is significantly higher than that of green, red, or yellow. Take particular note of the wavelength 1200 nm corresponding with the point where the curve drops to the horizontal axis. This is the highest wavelength that will provide photons with sufficient energy to liberate electrons in the silicon material. In other words, at this wavelength the energy associated with the incident light is just enough to release an electron-hole pair. Any photon associated with longer wavelengths will not have sufficient energy associated with it to release an electron and will simply contribute to the heating of the solar cell.

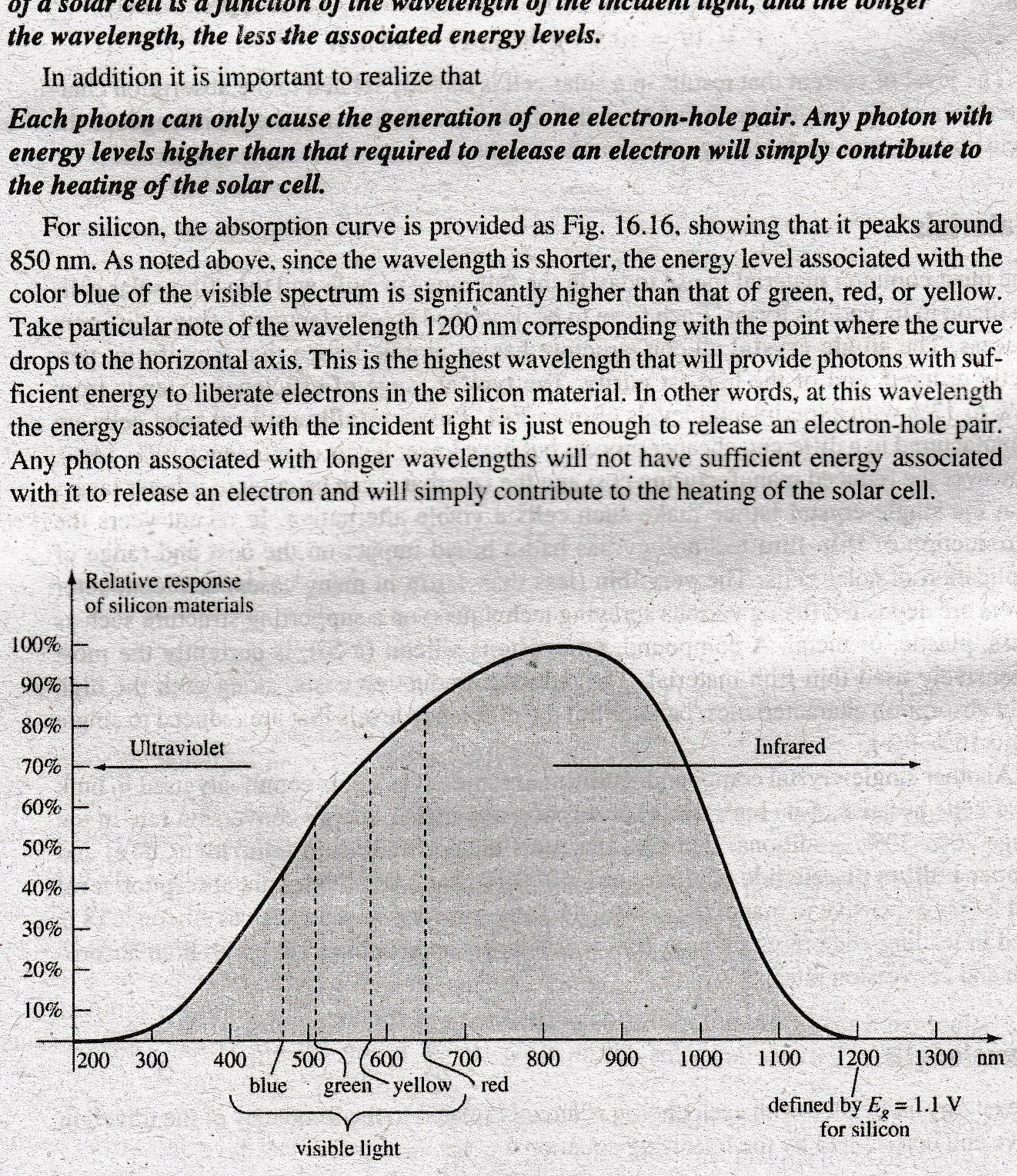

FIG. 16.16
Relative response of silicon versus the wavelength of the incident light.

Light Intensity

The third factor of major importance in the design of solar cells is the light intensity. The more intense the incident light, the greater the number of photons and resulting number of released electron-hole pairs. Light intensity is a measure of the amount of luminuous flux falling on a particular surface area. Luminous flux is normally measured in lumens (lm) or watts. The two units are related by

$$\boxed{1 \text{ lumen} = 1 \text{ lm} = 1.496 \times 10^{-10} \text{ W}} \qquad \textbf{(16.8)}$$

The light intensity is normally measured in lm/ft, footcandles (fc), or W/m, where

$$\boxed{1 \text{ lm/ft}^2 = 1\,fc = 1.609 \times 10^{-9} \text{ W/m}^2} \qquad \textbf{(16.9)}$$

As noted earlier in this section the light intensity of the sun at sea level is about 100 mW/cm^2 or 1 kW/m^2, which gives us a good idea of the maximum levels that can be expected from the sun.

Current Maximum Levels of Efficiency

In recent years solar cell efficiencies at research institutes have passed the 40% plateau. In fact in 2011 an efficiency level of 43.5% was achieved. For thin-film technologies the maximum remains about 20%, whereas single-crystal GaAs cells are at 29% and single-crystal Si at 25%.

Applications

In Fig. 16.17 a commercially available Edmund Scientific Multi-Volt Output Solar can be used to provide a solar output of 3 V at 200 mA, 6 V at 100 mA, 9 V at 50 mA, and 12 V at 50 mA. Assuming a terminal voltage of 0.5 V for each cell the 3-V level would require six cells in a series, the 6-V level would require 12 cells in a series, and so on. The switch position will simply select which series combination of cells is part of the output voltage. The supply can be used to charge mobile phones, MP3 players, flashlights, and video games. The current levels are not sufficiently high to charge a 12-V car battery, which is charged by currents in the ampere range. Take note of the relatively small size of the unit for its range of applications.

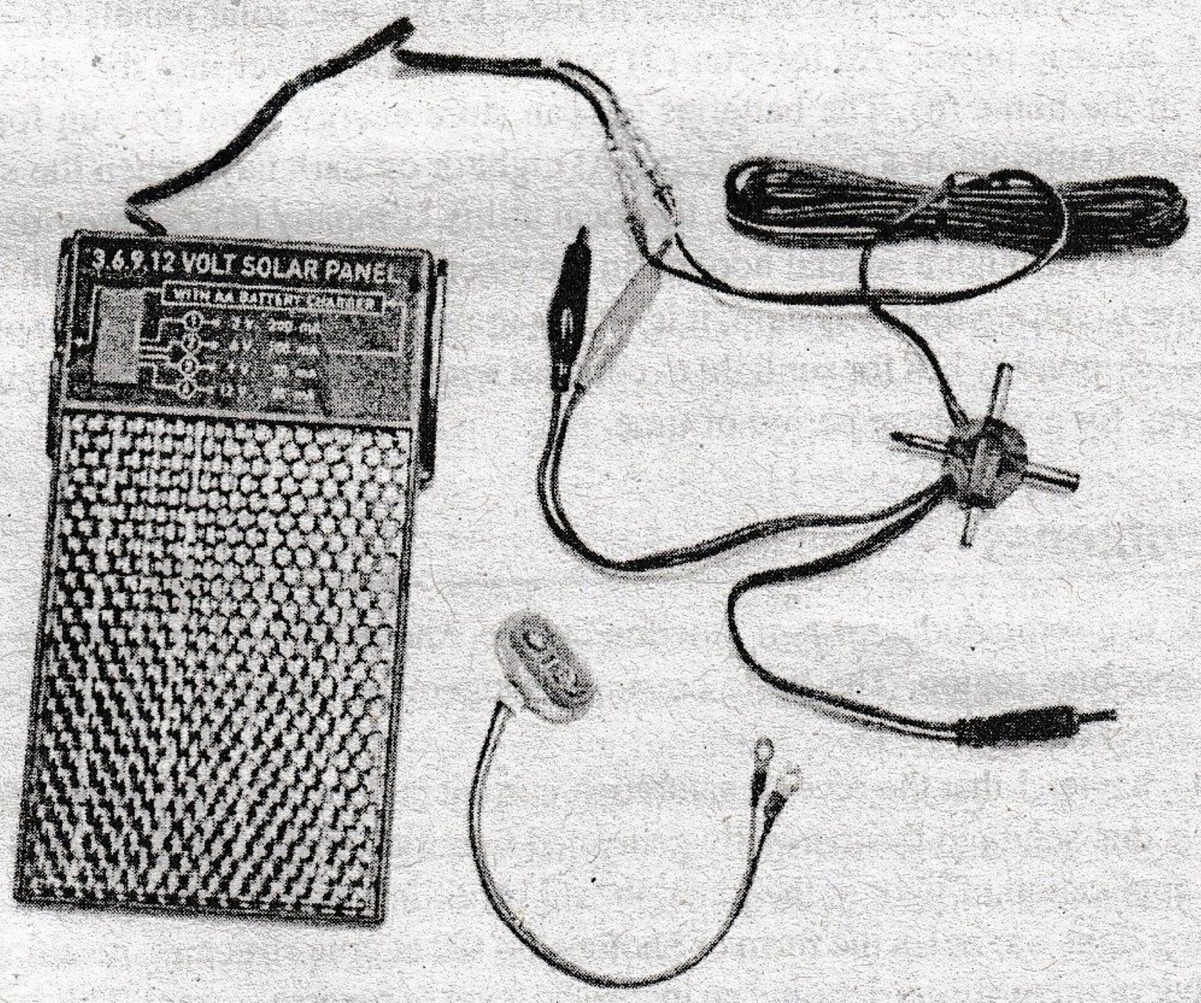

FIG. 16.17
Ednund Scientific multi-volt output solar panel.
(Photo by Dan Trudden/Pearson.)

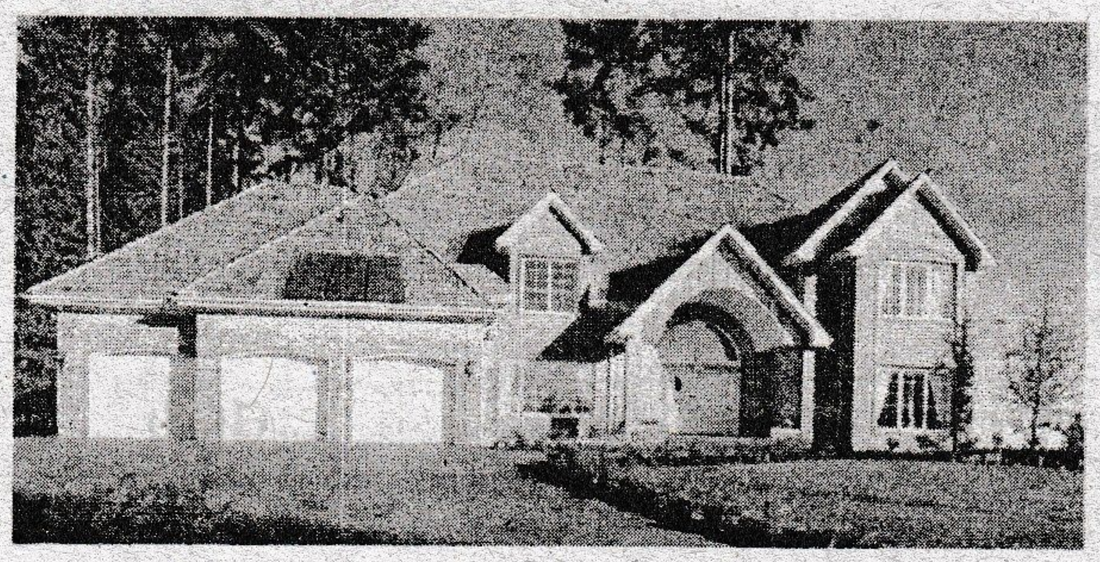

(a)

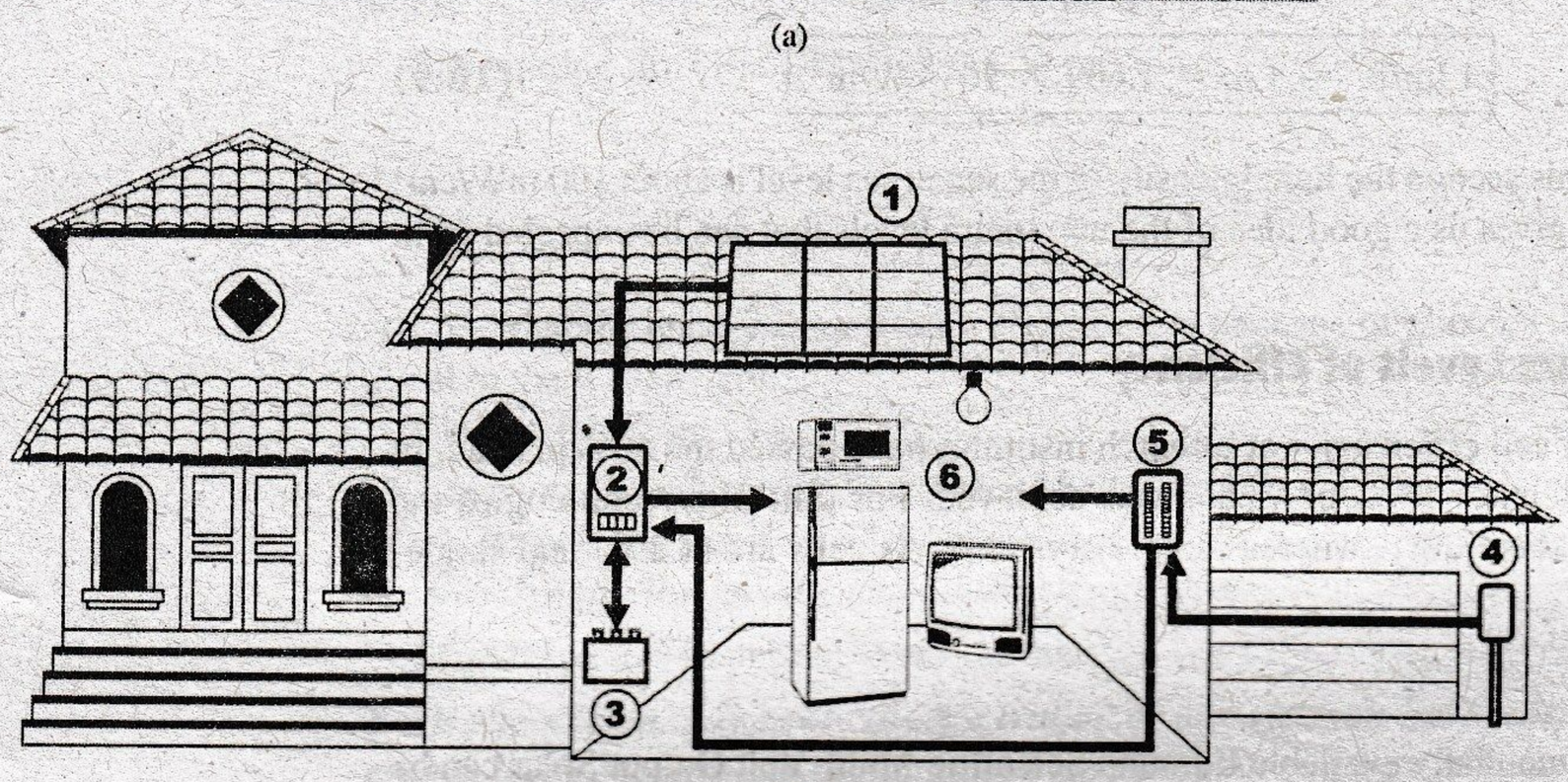

(b)

FIG. 16.18

Solar System: (a) panels on roof of garage; (b) system operation.

(Courtesy of SolarDirect.com)

Thin-film solar cell panels have led to widespread use of solar panels in the home. The solar panels appearing on the roof of the home of Fig. 16.18a are sufficient in power to run an energy-efficient refrigerator for 24 hours a day, while simultaneously running a color TV for 7 hours, a microwave for 15 minutes, a 60-W bulb for 10 hours, and an electric clock for 10 hours. The basic system operates as shown in Fig. 16.18b. The solar panels (1) convert sunlight into dc electric power. An inverter (2) converts the dc power into the standard ac power for use in the home (6). The batteries (3) can store energy from the sun for use if there is insufficient sunlight or a power failure. At night or on dark days when the demand exceeds the solar panel and battery supply, the local utility company (4) can provide power to the appliances (6) through a special hookup in the electrical panel (5). Although there is an initial expense to setting up the system, it is vitally important to realize that the source of energy is free—no monthly bill for sunlight to contend with—and will provide a significant amount of energy for a very long period of time.

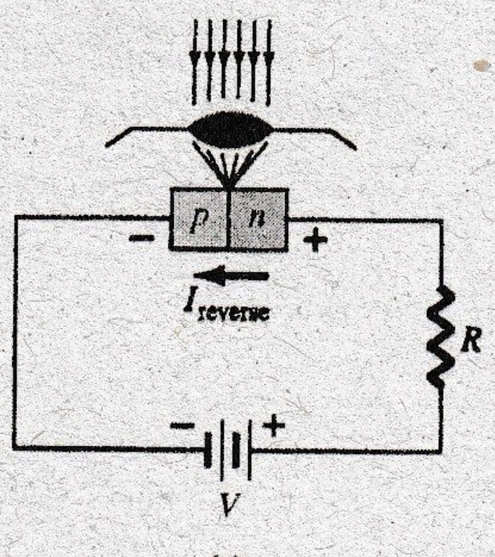

(a)

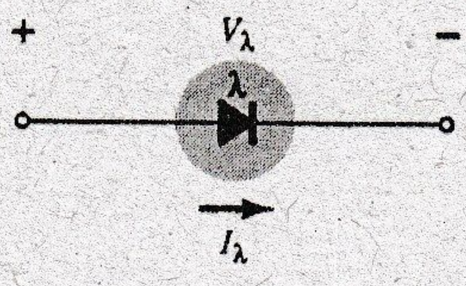

(b)

FIG. 16.19

Photodiode: (a) basic biasing arrangement and construction; (b) symbol.

16.5 PHOTODIODES

The photodiode is a semiconductor *p–n* junction device whose region of operation is limited to the reverse-bias region. The basic biasing arrangement, construction, and symbol for the device appear in Fig. 16.19.

Recall from Chapter 1 that the reverse saturation current is normally limited to a few microamperes. It is due solely to the thermally generated minority carriers in the *n*- and *p*-type materials. The application of light to the junction will result in a transfer of energy from the incident traveling light waves (in the form of photons) to the atomic structure, resulting in an increased number of minority carriers and an increased level of reverse current. This is clearly shown in Fig. 16.20 for different intensity levels. The *dark* current is that current that will exist with no applied illumination. Note that the current will only return to zero with a positive applied bias equal to V_T. In addition, Fig. 16.19a demonstrates the use of a lens to concentrate the light on the junction region. Commercially available photodiodes appear in Fig. 16.21.

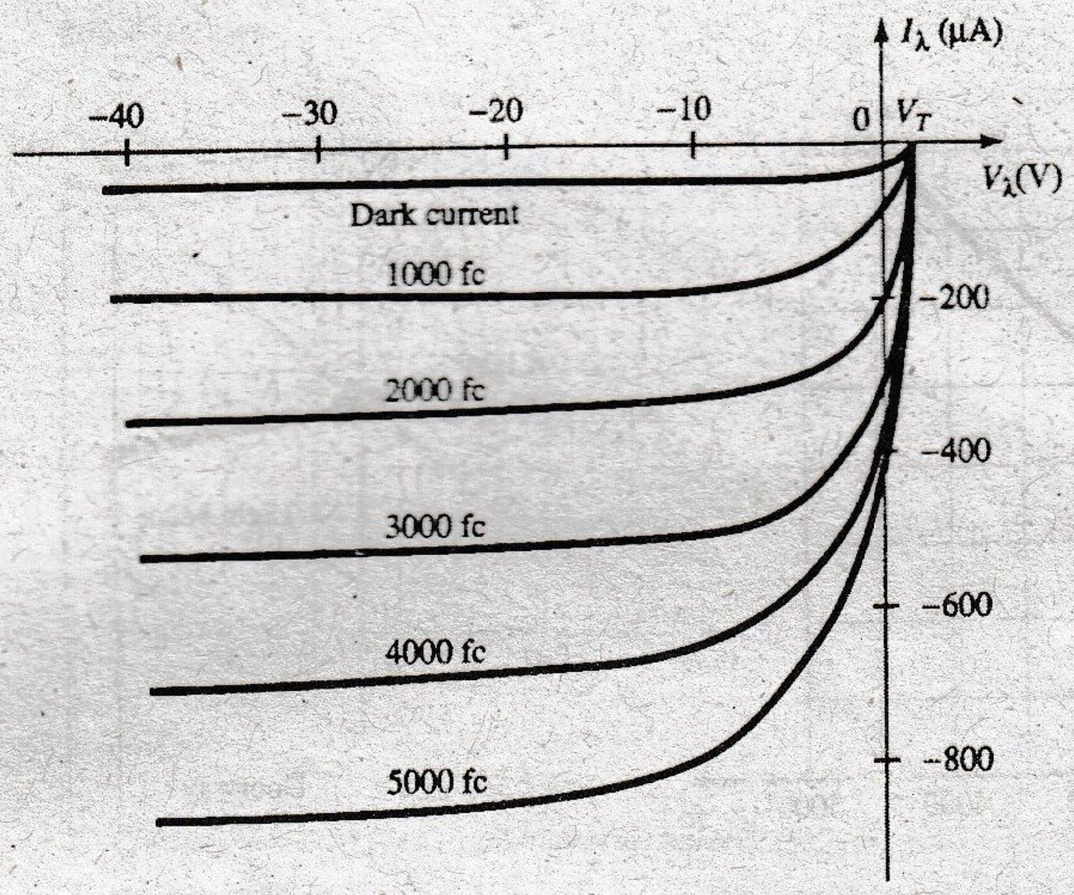

FIG. 16.20
Photodiode characteristics.

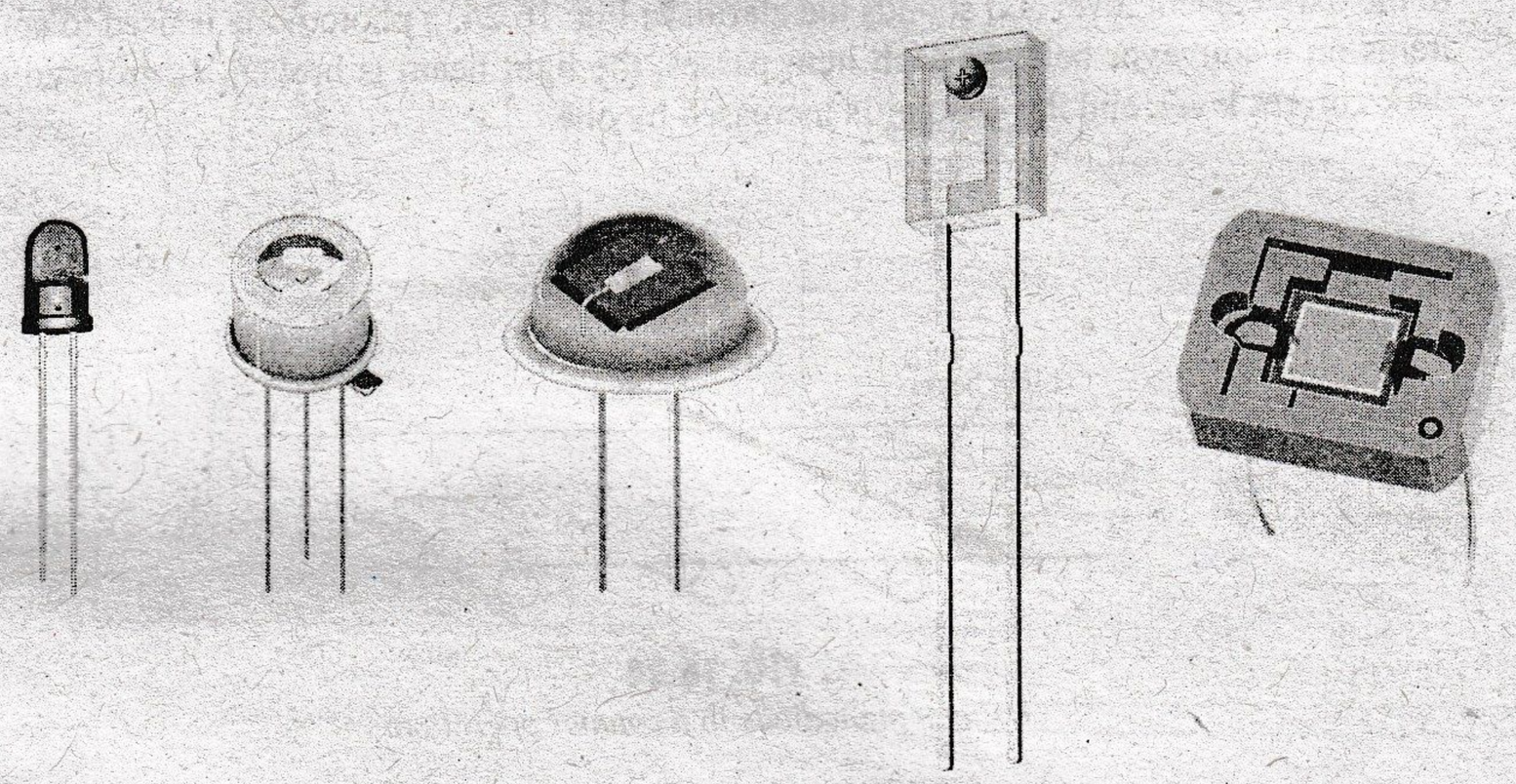

FIG. 16.21
Photodiodes

The almost equal spacing between the curves for the same increment in luminous flux reveals that the reverse current and the luminous flux are almost linearly related. In other words, an increase in light intensity will result in a similar increase in reverse current. A plot of the two to show this linear relationship appears in Fig. 16.22 for a fixed voltage V_λ of 20 V. On a relative basis, we can assume that the reverse current is essentially zero in the absence of incident light. Since the rise and fall times (change-of-state parameters) are very small for this device (in the nanosecond range), the device can be used for high-speed counting or switching applications. Germanium encompasses a wider spectrum of wavelengths than Si, making it suitable for incident light in the infrared region as provided by lasers and IR (infrared) light sources, to be described shortly. Germanium has a higher dark current than Si, but it also has a higher level of reverse current. The level of current generated by the incident light on a photodiode is not such that it could be used as a direct control, but it can be amplified for this purpose.

Applications

In Fig. 16.23, the photodiode is employed in an alarm system. The reverse current I_λ will continue to flow as long as the light beam is not broken. If the beam is interrupted, I_λ drops

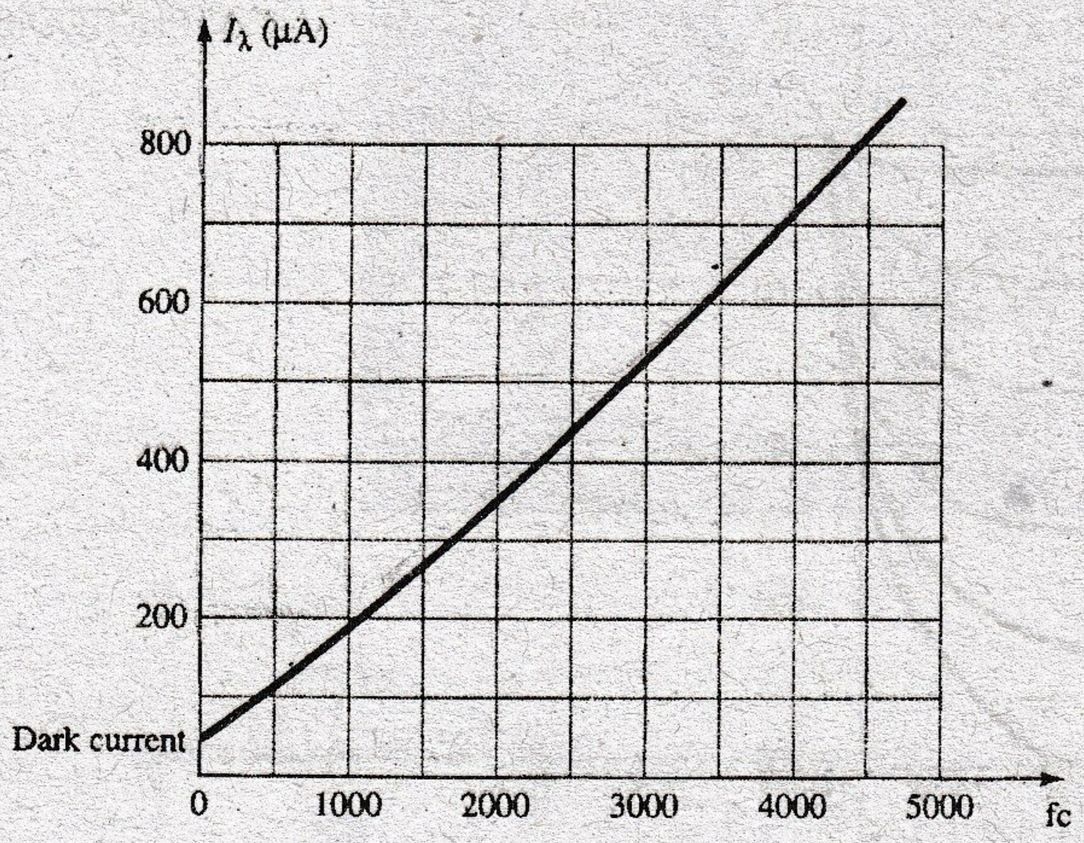

FIG. 16.22

I_λ (μA) versus f_C (at V_λ = 20 V) for the photodiode of Fig. 16.20.

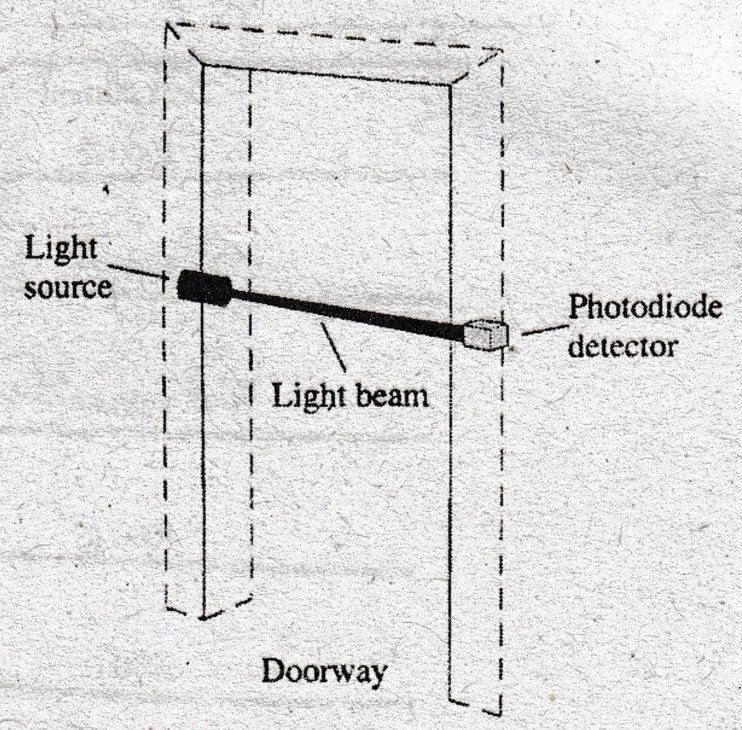

FIG. 16.23

Using a photodiode in an alarm system.

to the dark current level and sounds the alarm. In Fig. 16.24, a photodiode is used to count items on a conveyor belt. As each item passes, the light beam is broken, I_λ drops to the dark current level, and the counter is increased by one.

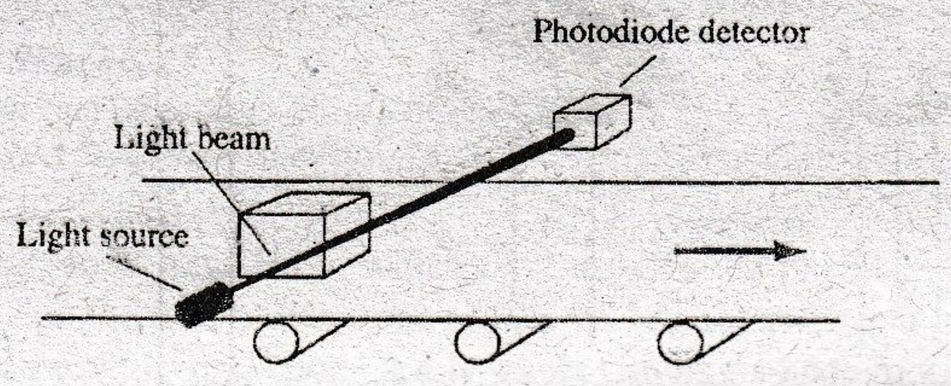

FIG. 16.24

Using a photodiode in a counter operation.

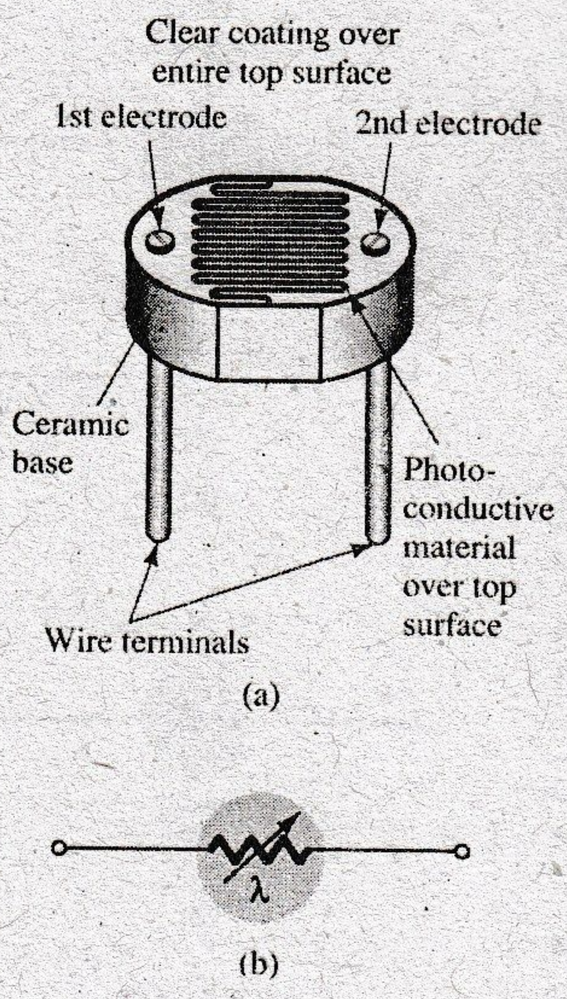

FIG. 16.25

Photoconductive cell: (a) construction; (b) symbol.

16.6 PHOTOCONDUCTIVE CELLS

The photoconductive cell is a two-terminal semiconductor device whose terminal resistance varies (linearly) with the intensity of the incident light. For obvious reasons, it is frequently called a *photoresistive device*. The typical construction of a photoconductive cell is provided in Fig. 16.25 with the most common graphical symbol.

The photoconductive materials most frequently used include cadmium sulfide (CdS) and cadmium selenide (CdSe). The peak spectral response occurs at approximately 5100 Å for CdS and at 6150 Å for CdSe. The response time of CdS units is about 100 ms and of CdSe cells is 10 ms. The photoconductive cell does not have a junction like the photodiode. A thin layer of the material connected between terminals is simply exposed to the incident light energy.

As the illumination on the device increases in intensity, the energy state of a larger number of electrons in the structure will also increase because of the increased availability of the photon packages of energy. The result is an increasing number of relatively "free" electrons in the structure and a decrease in the terminal resistance. The sensitivity curve for a typical photoconductive device appears in Fig. 16.26. Note the linearity (when plotted using a log–log scale) of the resulting curve and the large change in resistance (100 kΩ → 100 Ω) for the indicated change in illumination.

To see the wealth of material available on each device from manufacturers, consider the CdS (cadmium sulfide) photoconductive cell described in Fig. 16.27. Note again the concern with temperature and response time.

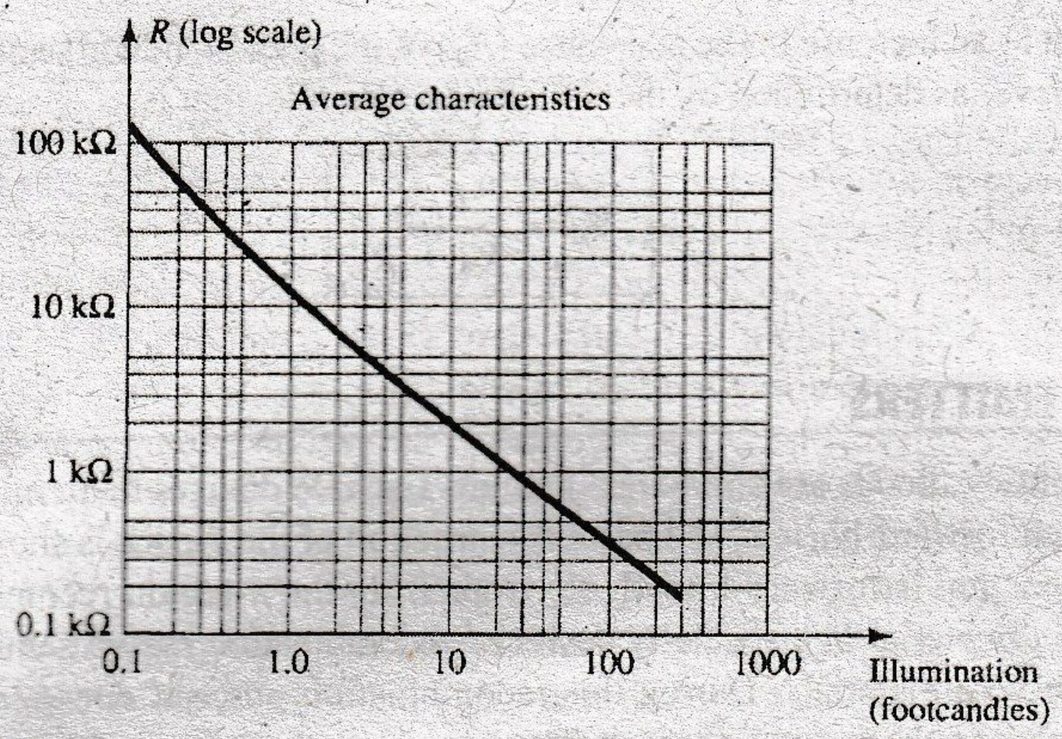

FIG. 16.26
Photoconductive cell-terminal characteristics.

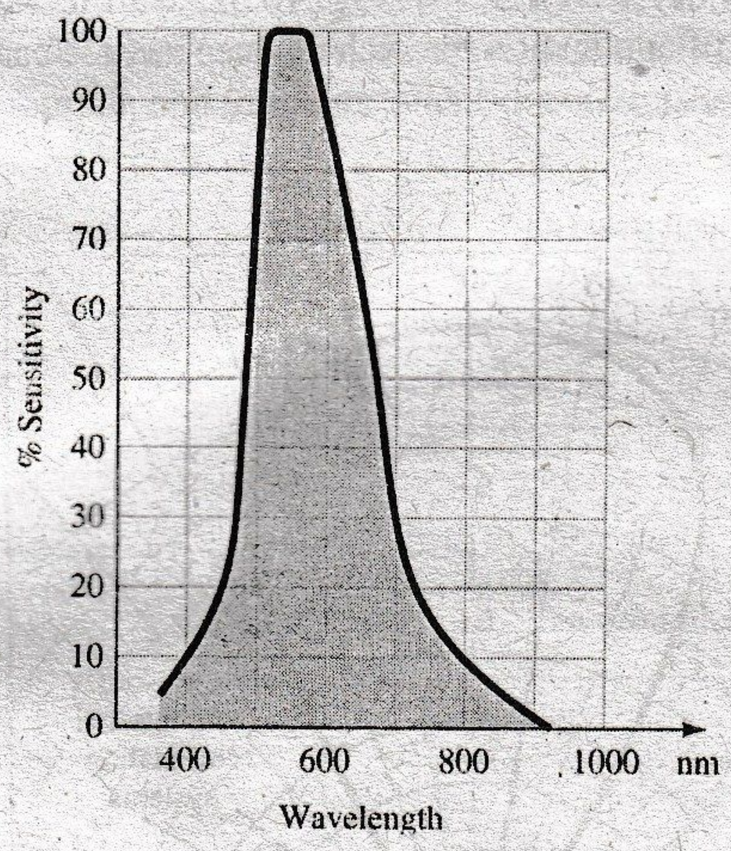

Variation of Conductance with Temperature and Light

Footcandles	*0.01*	*0.1*	*1.0*	*10*	*100*
Temperature	*% Conductance*				
−25°C	103	104	104	102	106
0	98	102	102	100	103
25°C	100	100	100	100	100
50°C	98	102	103	104	99
75°C	90	106	108	109	104

Response Time versus Light

Footcandles	*0.01*	*0.1*	*1.0*	*10*	*100*
Rise (seconds)	0.5	0.095	0.022	0.005	0.002
Decay (seconds)	0.125	0.021	0.005	0.002	0.001

FIG. 16.27
Characteristics of a Clairex CdS photoconductive cell.

Application

One rather simple but interesting application of the device appears in Fig. 16.28. The purpose of the system is to maintain V_o at a fixed level even though V_i may fluctuate from its rated value. As indicated in the figure, the photoconductive cell, bulb, and resistor all form part of this voltage-regulator system. If V_i should drop in magnitude for any of a number of reasons, the brightness of the bulb would also decrease. The decrease in illumination

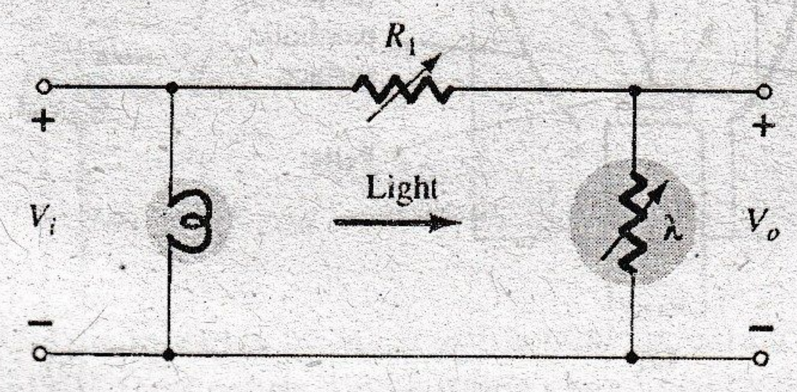

FIG. 16.28
Voltage regulator employing a photoconductive cell.

would result in an increase in the resistance (R_λ) of the photoconductive cell to maintain V_o at its rated level as determined by the voltage-divider rule, that is,

$$V_o = \frac{R_\lambda V_i}{R_\lambda + R_1} \tag{16.10}$$

16.7 IR EMITTERS

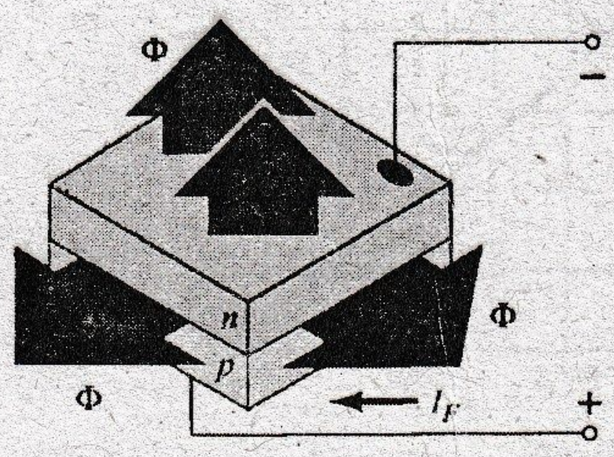

FIG. 16.29
General structure of a semiconductor IR-emitting diode.

Infrared-emitting diodes are solid-state gallium arsenide devices that emit a beam of radiant flux when forward-biased. The basic construction of the device is shown in Fig. 16.29. When the junction is forward-biased, electrons from the *n*-region recombine with excess holes of the *p*-material in a specially designed recombination region sandwiched between the *p*- and *n*-type materials. During this recombination process, energy is radiated away from the device in the form of photons. The generated photons are either reabsorbed in the structure or leave the surface of the device as radiant energy, as shown in Fig. 16.29.

The radiant flux in milliwatts versus the dc forward current for a typical device appears in Fig. 16.30. Note the almost linear relationship between the two. An interesting pattern for such devices is provided in Fig. 16.31. Note the very narrow pattern for devices with an internal collimating system. One such device appears in Fig. 16.32, with its internal construction and graphical symbol. Areas of application for such devices include card and paper-tape readers, shaft encoders, data-transmission systems, and intrusion alarms.

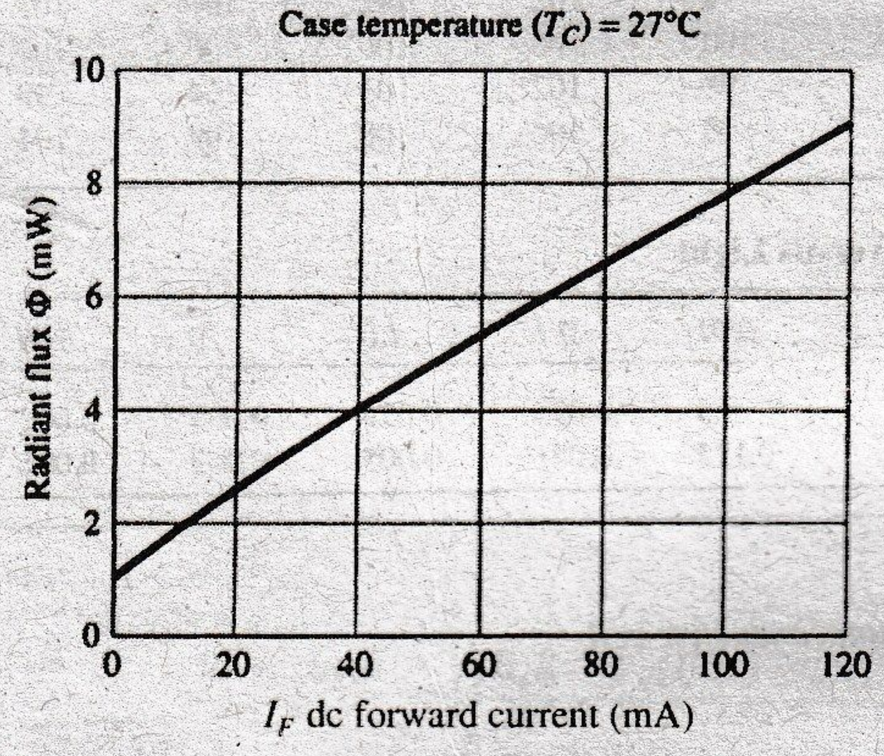

FIG. 16.30
Typical radiant flux versus dc forward current for an IR-emitting diode.

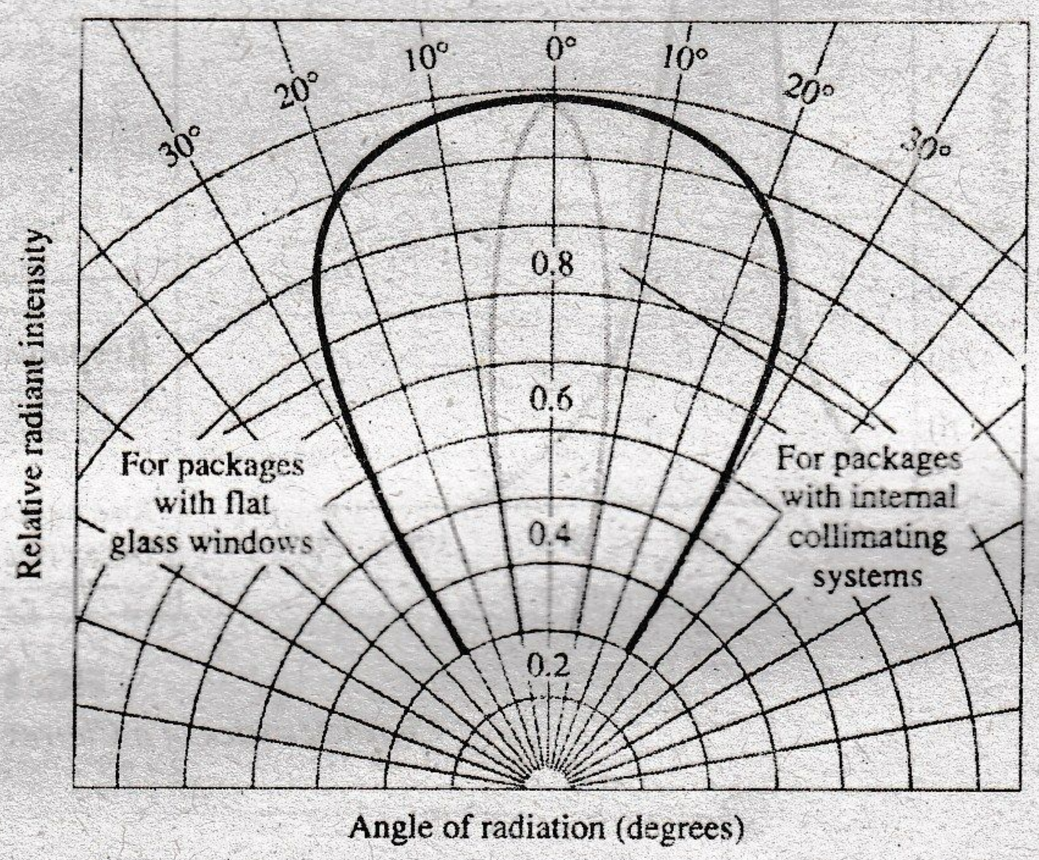

FIG. 16.31
Typical radiant intensity patterns of an IR-emitting diode.

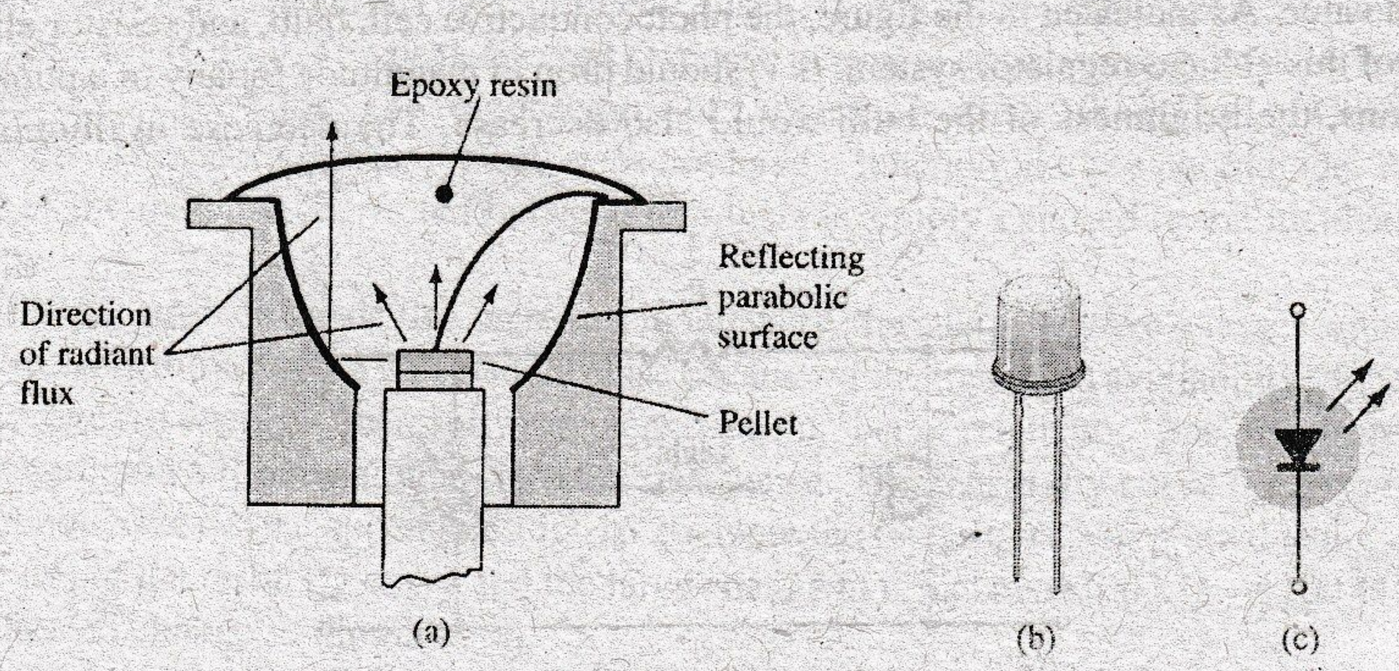

FIG. 16.32
IR-emitting diode: (a) construction; (b) photo; (c) symbol.

16.8 LIQUID-CRYSTAL DISPLAYS

The liquid-crystal display (LCD) has the distinct advantage of having a lower power requirement than the LED, typically on the order of microwatts for the display, compared to the order of milliwatts for LEDs. It does, however, require an external or internal light source, and is limited to a temperature range of about 0°C to 60°C. Lifetime is an area of concern because LCDs can chemically degrade. The types of unit of major interest are field-effect and dynamic-scattering units. Each will be covered in some detail in this section.

A liquid crystal is a material (normally organic for LCDs) that flows like a liquid but whose molecular structure has some properties normally associated with solids. For light-scattering units, the greatest interest is in *nematic liquid crystal,* which has the crystal structure shown in Fig. 16.33. The individual molecules have a rodlike appearance as shown in the figure. The indium oxide conducting surface is transparent, and under the condition shown in the figure, incident light will simply pass through and the liquid-crystal structure will appear clear. If a voltage (for commercial units the threshold level is usually between 6 V and 20 V) is applied across the conducting surfaces, as shown in Fig. 16.34, the molecular arrangement is disturbed, with the result that regions are established with different indices of refraction. The incident light is therefore reflected in different directions at the interface between regions of different indices of refraction (referred to as *dynamic scattering*—first studied by RCA in 1968), with the result that the scattered light has a frosted-glass appearance. Note in Fig. 16.34, however, that the frosted look occurs only where the conducting surfaces are opposite each other; the remaining areas remain translucent.

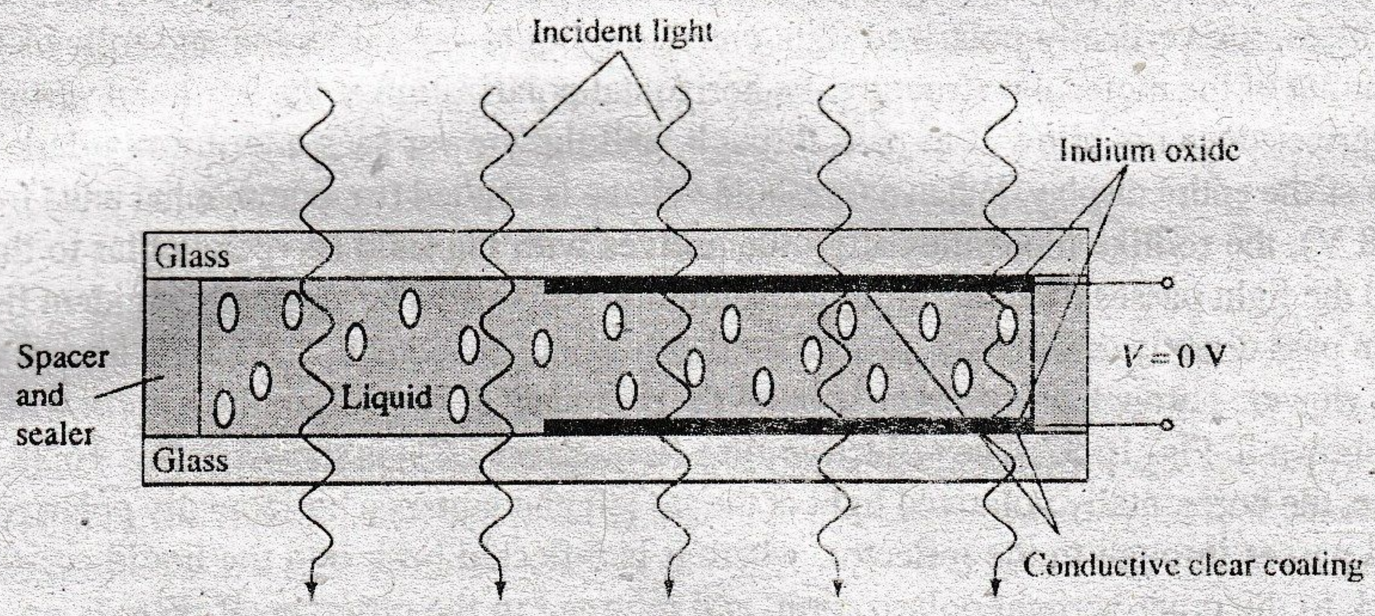

FIG. 16.33
Nematic liquid crystal with no applied bias.

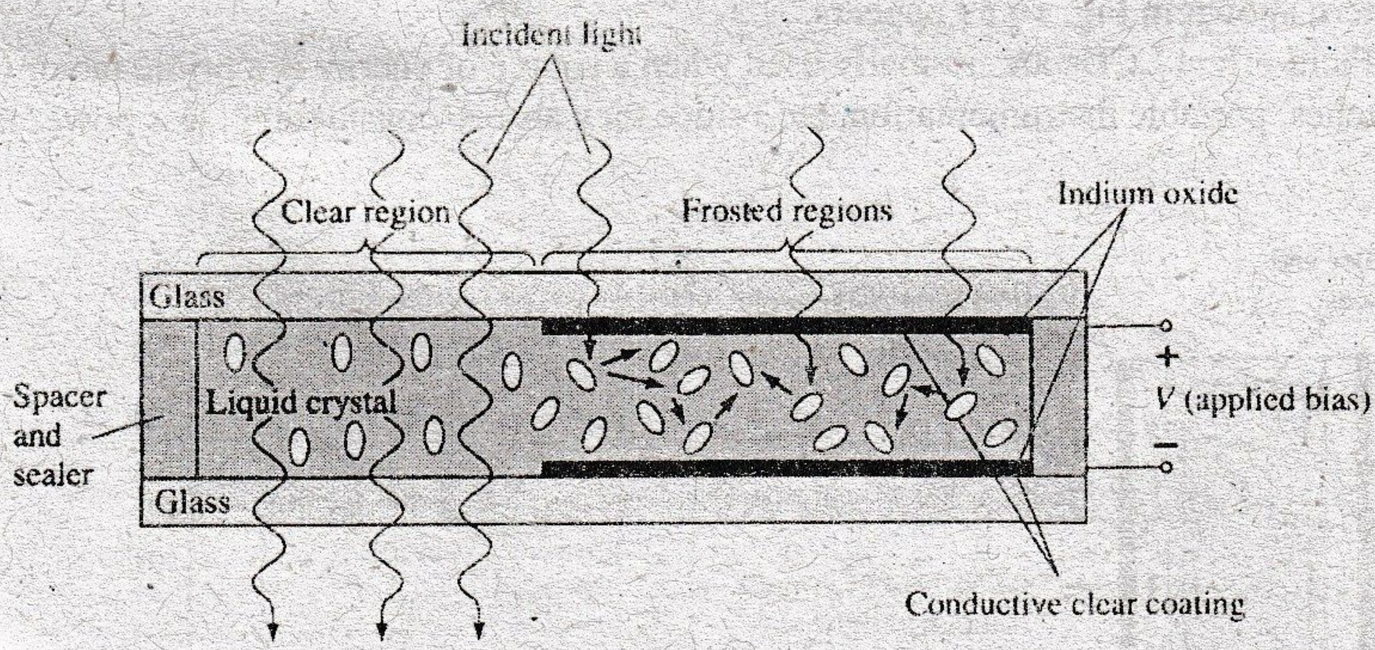

FIG. 16.34
Nematic liquid crystal with applied bias.

A numeral on an LCD display may have the segmented appearance shown in Fig. 16.35. The black area is actually a clear conducting surface connected to the terminals below for external control. Two similar masks are placed on opposite sides of a sealed, thick layer of liquid-crystal material. If the number 2 were required, the terminals 8, 7, 3, 4, and 5 would

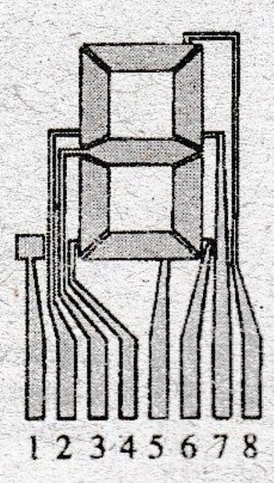

FIG. 16.35
LCD eight-segment digit display.

be energized, and only those regions would be frosted, whereas the other areas would remain clear.

As indicated earlier, the LCD does not generate its own light, but depends on an external or internal source. Under dark conditions, it would be necessary for the unit to have its own internal light source either behind or to the side of the LCD. During the day, or in lighted areas, a reflector can be put behind the LCD to reflect the light back through the display for maximum intensity. For optimum operation, watch manufacturers use a combination of the transmissive (own light source) and reflective modes called *transflective* operation.

The *field-effect* or *twisted nematic* LCD has the same segmented appearance and thin layer of encapsulated liquid crystal, but its mode of operation is very different. Similar to the dynamic-scattering LCD, the field-effect LCD can be operated in the reflective or the transmissive mode with an internal source. The transmissive display appears in Fig. 16.36. The internal light source is on the right, and the viewer is on the left. This figure is most noticeably different from Fig. 16.33 in that there is an addition of a *light polarizer*. Only the vertical component of the entering light on the right can pass through the vertical-light polarizer on the right. In the field-effect LCD, either the clear conducting surface to the right is chemically etched or an organic film is applied to orient the molecules in the liquid crystal in the vertical plane, parallel to the cell wall. Note the rods to the far right in the liquid crystal. The opposite conducting surface is also treated to ensure that the molecules are 90° out of phase in the direction shown (horizontal) but still parallel to the cell wall. In between the two walls of the liquid crystal there is a general drift from one polarization to the other, as shown in the figure. The left-hand light polarizer is also such that it permits the passage of only the vertically polarized incident light. If there is no applied voltage to the conducting surfaces, the vertically polarized light enters the liquid-crystal region and follows the 90° bending of the molecular structure. Its horizontal polarization at the left-hand vertical light polarizer does not allow it to pass through, and the viewer sees a uniformly dark pattern across the entire display. When a threshold voltage is applied (for commercial units from 2 V to 8 V), the rodlike molecules align themselves with the field (perpendicular to the wall) and the light passes directly through without the 90° shift. The vertically incident light can then pass directly through the second vertically polarized screen, and a light area is seen by the viewer. Through proper excitation of the segments of each digit, the pattern will appear as shown in Fig. 16.37. The reflective-type field-effect LCD is shown in Fig. 16.38. In this case, the horizontally polarized light at the far left encounters a horizontally polarized filter and passes through to the reflector, where it is reflected back into the liquid crystal, bent back to the other vertical polarization, and returned to the observer. If there is no applied voltage, there is a uniformly lit display. The application of a voltage results in a vertically incident light encountering a horizontally polarized filter at the left, through which it will not be able to pass, and so it will be reflected. A dark area results on the crystal, and the pattern shown in Fig. 16.39 appears.

Field-effect LCDs are normally used when a source of energy is a prime factor (e.g., in watches, portable instrumentation, etc.) since they absorb considerably less power than the

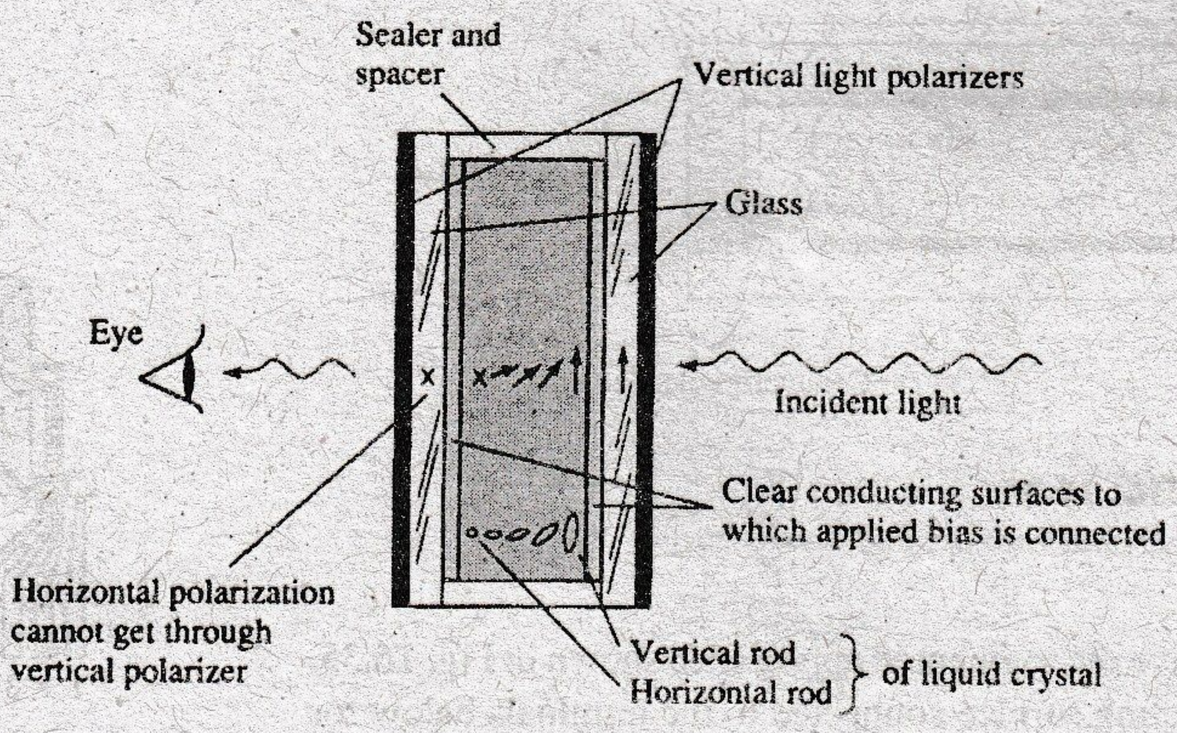

FIG. 16.36
Transmissive field-effect LCD with no applied bias.

FIG. 16.37
Reflective-type LCD.

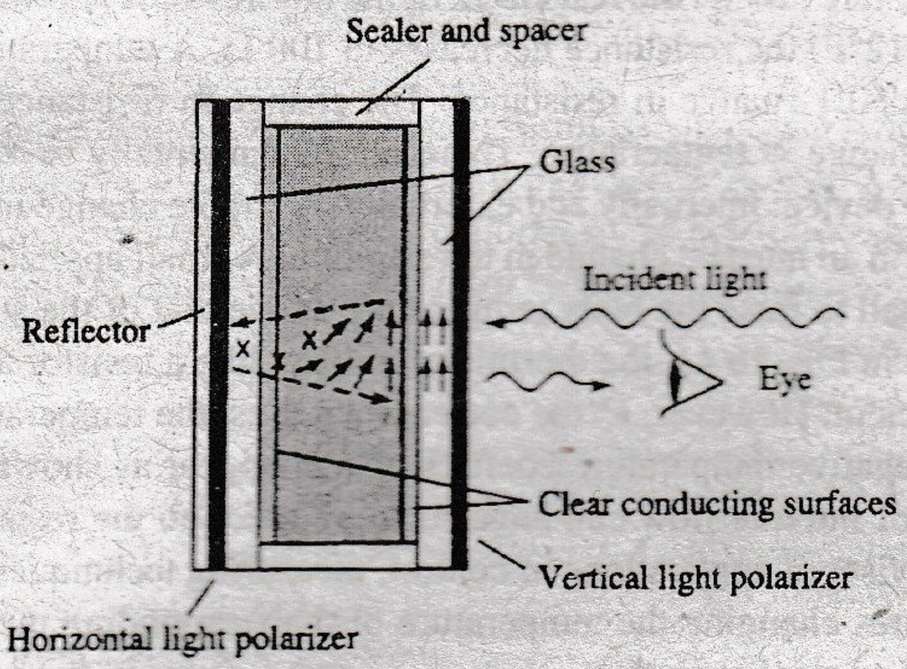

FIG. 16.38
Reflective field-effect LCD with no applied bias.

FIG. 16.39
Transmissive-type LCD.

light-scattering types—the microwatt range compared to the low-milliwatt range. The cost is typically higher for field-effect units, and their height is limited to about 2 in., whereas light-scattering units are available up to 8 in. in height.

A further consideration in displays is turn-on and turn-off time. LCDs are characteristically much slower than LEDs. LCDs typically have response times in the range 100 ms to 300 ms, whereas LEDs are available with response times below 100 ns. However, there are numerous applications, such as in a watch, where the difference between 100 ns and 100 ms ($\frac{1}{10}$ of a second) is of little consequence. For such applications, the lower power demand of LCDs is a very attractive characteristic. The lifetime of LCD units is steadily increasing beyond the 10,000+-hour limit. Since the color generated by LCD units is dependent on the source of illumination, there is a greater range of color choice.

16.9 THERMISTORS

The thermistor is, as the name implies, a temperature-sensitive resistor; that is, its terminal resistance is related to its body temperature. It is not a junction device and is constructed of germanium, silicon, or a mixture of oxides of cobalt, nickel, strontium, or manganese. The compound employed determines whether the device has a positive or a negative temperature coefficient.

The characteristics of a typical thermistor with a negative temperature coefficient are provided in Fig. 16.40, which also shows the commonly used symbol for the device. Note in

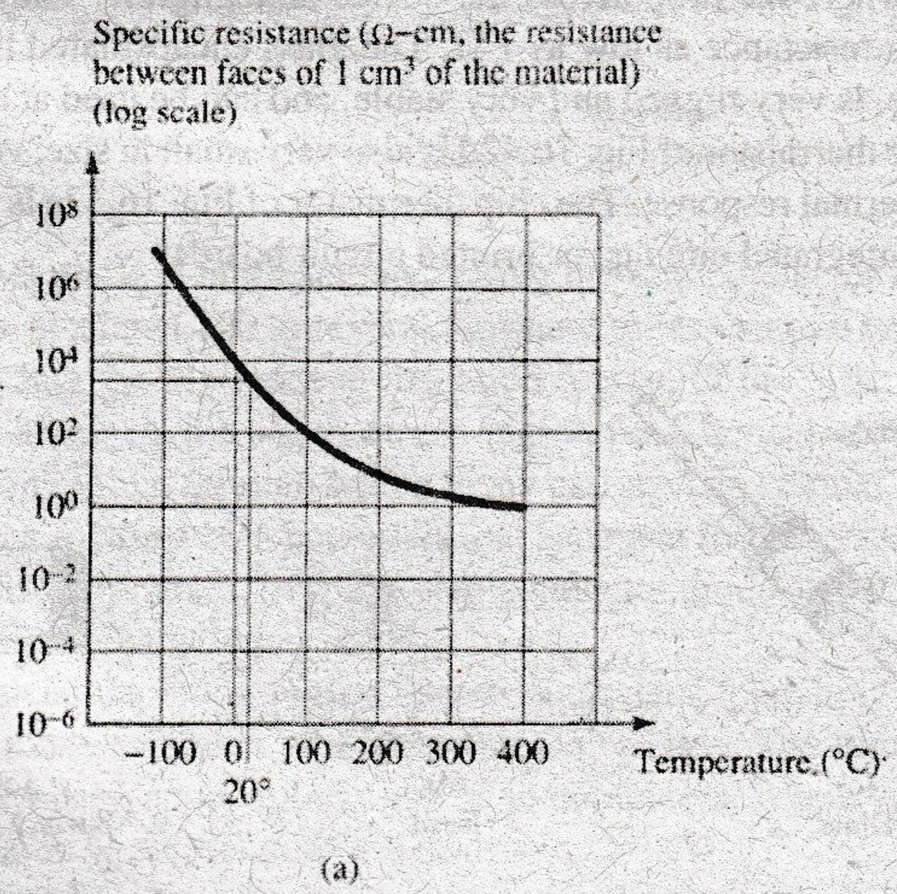

FIG. 16.40
Thermistor: (a) typical set of characteristics; (b) symbol.

particular that at room temperature (20°C) the resistance of the thermistor is approximately 5000 Ω, whereas at 100°C (212°F) the resistance decreases to 100 Ω. A temperature span of 80°C therefore results in a 50:1 change in resistance. The change in resistance is typically 3% to 5% per degree change in temperature. There are fundamentally two ways to change the temperature of the device: internally and externally. A simple change in current through the device will result in an internal change in temperature. A small applied voltage will result in a current too small to raise the body temperature above that of the surroundings. In this region, as shown in Fig. 16.41, the thermistor will act like a resistor and have a positive temperature coefficient. However, as the current increases, the temperature will rise to the point where the negative temperature coefficient will appear as shown in Fig. 16.41. The fact that the rate of internal flow can have such an effect on the resistance of the device introduces a wide vista of applications in control, measuring techniques, and so on. An external change requires changing the temperature of the surrounding medium or immersing the device in a hot or a cold solution.

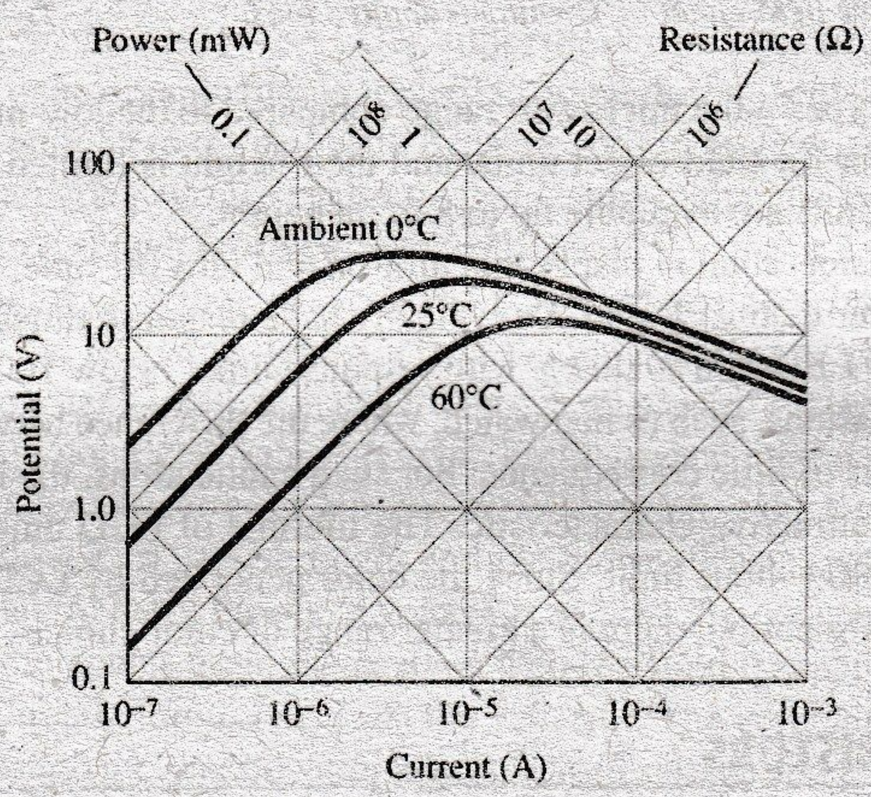

FIG. 16.41
Steady-state voltage–current characteristics of a thermistor.

A few of the most popular packaging techniques for U.S. sensor thermistor elements are provided in Fig. 16.42. The probe of Fig. 16.42a has a high stability factor and is rugged and very precise for applications ranging from laboratory applications to severe environmental conditions. The power thermistors of Fig. 16.42b have the unique ability to limit any in-rush current to an acceptable level until the capacitors are charged. The resistance of the device will then drop to a level where the drop across the device is negligible. They can handle currents up to 20 A with a resistance as low as 1 Ω. The glass encapsulated thermistor of Fig. 16.42c is small in size, is very rugged and very stable, and can be used at temperatures up to 300°C. The bead type thermistor of Fig. 16.42d is also very small in size, very accurate, and stable and has a fast thermal response. The chip thermistor of Fig. 16.42e is designed for use on hybrid substrates, integrated circuits, or printed circuit boards.

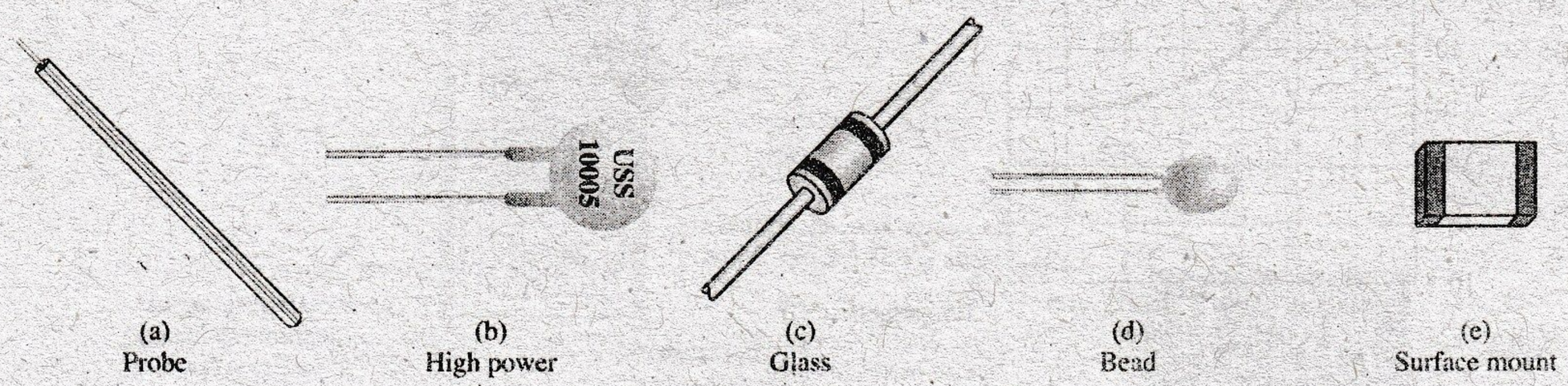

FIG. 16.42
Various types of packaging for U.S. sensor thermistors.

Application

A simple temperature-indicating circuit appears in Fig. 16.43. Any increase in the temperature of the surrounding medium will result in a decrease in the resistance of the thermistor and an increase in the current I_T. An increase in I_T will produce an increased movement deflection, which when properly calibrated will accurately indicate the higher temperature. The variable resistance was added for calibration purposes.

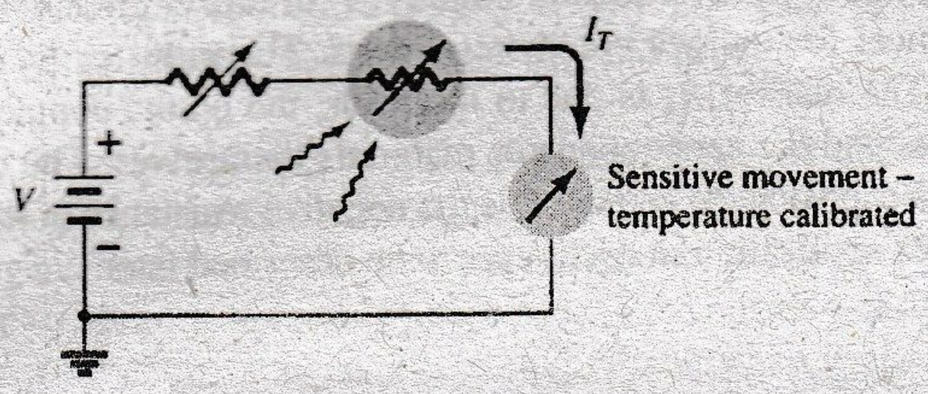

FIG. 16.43
Temperature-indicating circuit.

16.10 TUNNEL DIODES

The tunnel diode was first introduced by Leo Esaki in 1958. Its characteristics, shown in Fig. 16.44, are different from any diode discussed thus far in that it has a negative-resistance region. In this region, an increase in terminal voltage results in a reduction in diode current.

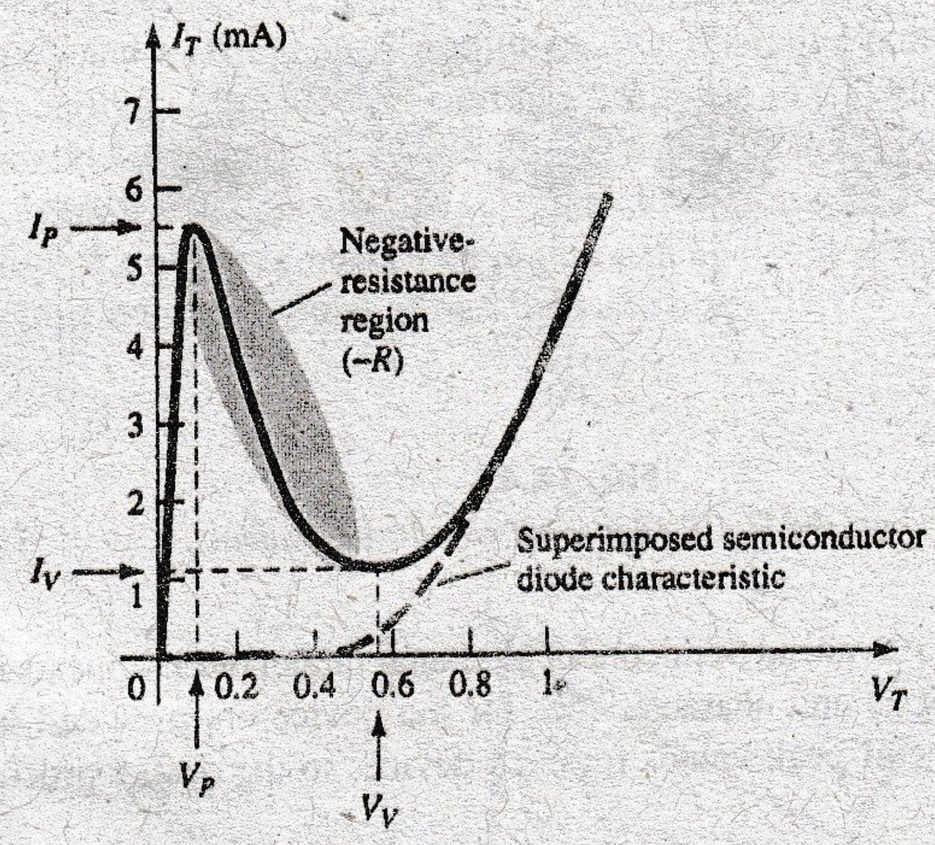

FIG. 16.44
Tunnel diode characteristics.

The tunnel diode is fabricated by doping the semiconductor materials that will form the p–n junction at a level 100 to several thousand times that of a typical semiconductor diode. This results in a greatly reduced depletion region, of the order of magnitude of 10^{-6} cm, or typically about $\frac{1}{100}$ the width of this region for a typical semiconductor diode. It is this thin depletion region, through which many carriers can "tunnel" rather than attempt to surmount, at low forward-bias potentials that accounts for the peak in the curve of Fig. 16.44. For comparison purposes, a typical semiconductor diode characteristic is superimposed on the tunnel-diode characteristic of Fig. 16.44.

This reduced depletion region results in carriers "punching through" at velocities that far exceed those available with conventional diodes. The tunnel diode can therefore be used in high-speed applications such as in computers, where switching times in the order of nanoseconds or picoseconds are desirable.

Recall from Section 1.15 that an increase in the doping level reduces the Zener potential. Note the effect of a very high doping level on this region in Fig. 16.44. The semiconductor

materials most frequently used in the manufacture of tunnel diodes are germanium and gallium arsenide. The ratio I_P/I_V is very important for computer applications. For germanium, it is typically 10:1, and for gallium arsenide, it is closer to 20:1.

The peak current I_P of a tunnel diode can vary from a few microamperes to several hundred amperes. The peak voltage, however, is limited to about 600 mV. For this reason, a simple VOM with an internal dc battery potential of 1.5 V can severely damage a tunnel diode if applied improperly.

The tunnel-diode equivalent circuit in the negative-resistance region is provided in Fig. 16.45, with the symbols most frequently employed for tunnel diodes. The values for the parameters are typical for today's commercial units. The inductor L_S is due mainly to the terminal leads. The resistor R_S is due to the leads, the ohmic contact at the lead–semiconductor junction, and the semiconductor materials themselves. The capacitance C is the junction diffusion capacitance, and the R is the negative resistance of the region. The negative resistance finds application in oscillators to be described later.

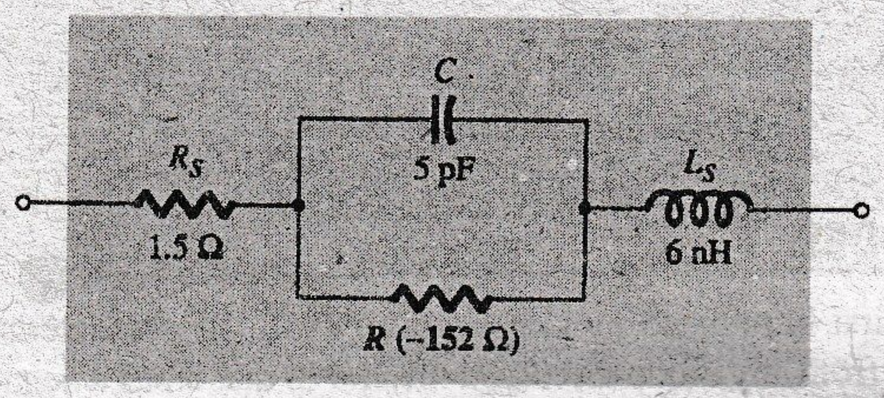

(a)

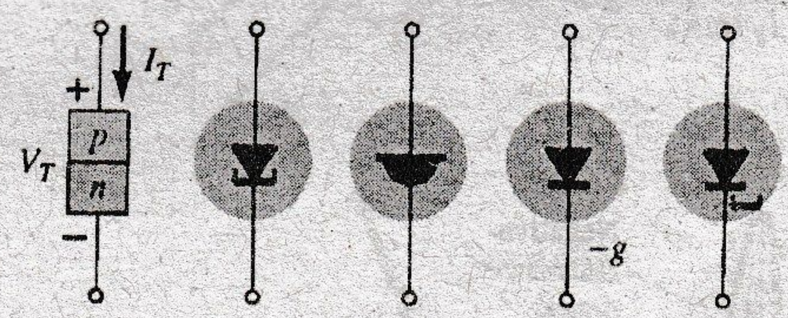

(b)

FIG. 16.45
Tunnel diode: (a) equivalent circuit; (b) symbols.

The packaging for an Advanced Semiconductor planar tunnel diode appears in Fig. 16.46 while the maximum ratings and characteristics for the device are provided in Fig. 16.47. Note that there is a range of peak values for each device, so the design process has to be

FIG. 16.46
Advanced Semiconductor planar tunnel diode.

Electrical Characteristics $T_C = 25°C$

Device	Symbol	Test Conditions	Min	Typ	Max	Units
ASTD1020	I_P		100		200	μA
ASTD2030			200		300	
ASTD3040			300		400	
ASTD1020	V_P				135	mV
ASTD2030					130	mV
ASTD3040					125	mV
ASTD1020	R_V	$f = 10$ GHz, $R_L = 10$ kΩ		−180		Ω
ASTD2030		$P_m = -20$ dBm		−130		Ω
ASTD3040				−80		Ω
All	R_S	$I = 10$ mA, $f = 100$ MHz		7		Ω

FIG. 16.47
Electrical characteristics for the Advanced Semiconductor planar tunnel diode of Fig. 16.46.

satisfactory for the full range of values. One can never tell which peak value will result for a particular device. This range of peak values is common for most tunnel diodes, so the designers are well aware of this concern. Interestingly enough, the valley voltage is fairly constant at about 0.13 V, which is significantly less than the typical turn-on voltage for a silicon diode. For this series of diodes, the negative resistance has a range of -80 to $-180\ \Omega$, which is a fairly large range for this important parameter. A number of tunnel diodes simply state a constant value such as $-250\ \Omega$ for a particular series.

Although the use of tunnel diodes in present-day high-frequency systems has been dramatically stalled because of the availability of manufacturing techniques for alternative devices, its simplicity, linearity, low power drain, and reliability ensure its continued life and application.

In Fig. 16.48, the chosen supply voltage and load resistance define a load line that intersects the tunnel diode characteristics at three points. Keep in mind that the load line is determined solely by the network and the characteristics of the device. The intersections at *a* and *b* are referred to as *stable* operating points, due to the positive-resistance characteristic. That is, at either of these operating points, a slight disturbance in the network will not set the network into oscillations or result in a significant change in the location of the *Q*-point. For instance, if the defined operating point is at *b*, a slight increase in supply voltage *E* will move the operating point up the curve since the voltage across the diode will increase. Once the disturbance has passed, the voltage across the diode and the associated diode current will return to the levels defined by the *Q*-point at *b*. The operating point defined by *c* is an *unstable* one because a slight change in the voltage across or current through the diode will result in the *Q*-point moving to either *a* or *b*. For instance, the slightest increase in *E* will cause the voltage across the tunnel diode to increase above its level at *c*. In this region, however, an increase in V_T will cause a decrease in I_T and a further increase in V_T. This increased level in V_T will result in a continuing decrease in I_T, and so on. The result is an increase in V_T and a change in I_T until the stable operating point at *b* is established. A slight drop in supply voltage would result in a transition to stability at point *a*. In other words, point *c* can be defined as the operating point using the load-line technique, but once the system is energized, it will eventually stabilize at location *a* or *b*.

The availability of a negative-resistance region can be put to good use in the design of oscillators, switching networks, pulse generators, and amplifiers.

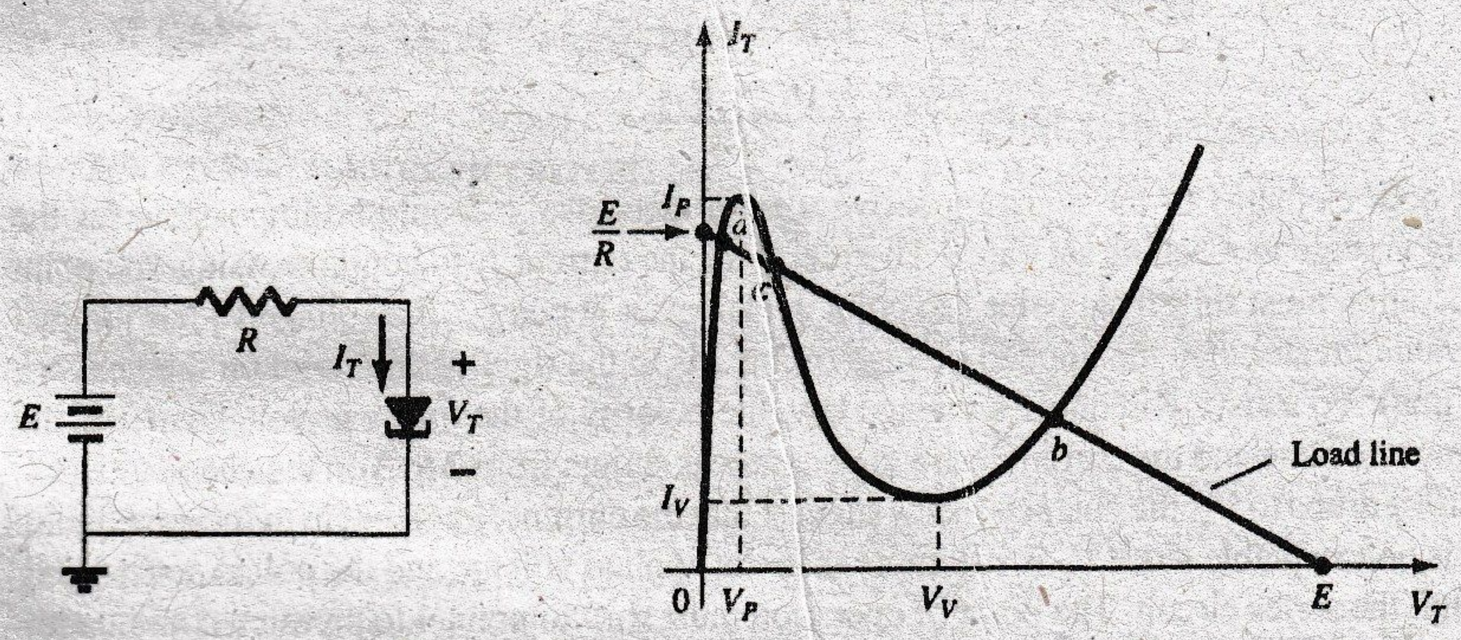

FIG. 16.48
Tunnel diode and resulting load line.

Applications

In Fig. 16.49a, a *negative-resistance oscillator* is shown as constructed using a tunnel diode. The choice of network elements is designed to establish a load line such as shown in Fig. 16.49b. Note that the only intersection with the characteristics is in the unstable negative-resistance region—a stable operating point is not defined. When the power is turned on, the terminal voltage of the supply will build up from 0 V to a final value of *E* volts. Initially, the current I_T will increase from 0 mA to I_P, resulting in a storage of energy in the inductor in the form of a magnetic field. However, once I_P is reached, the diode

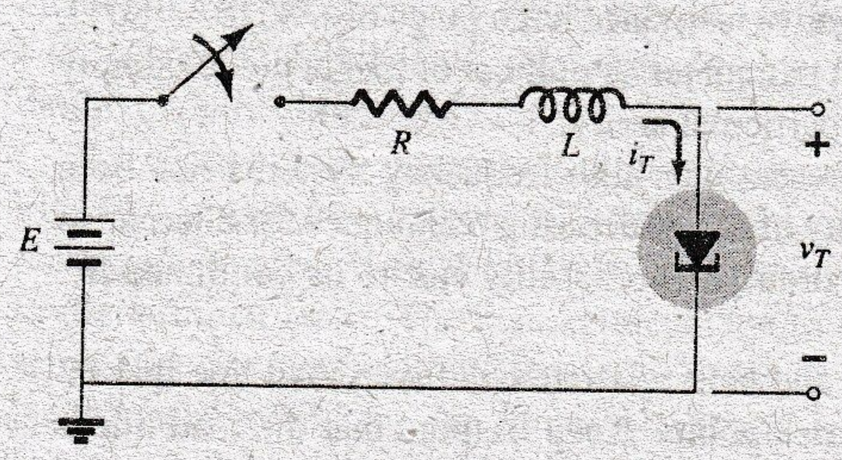

(a)

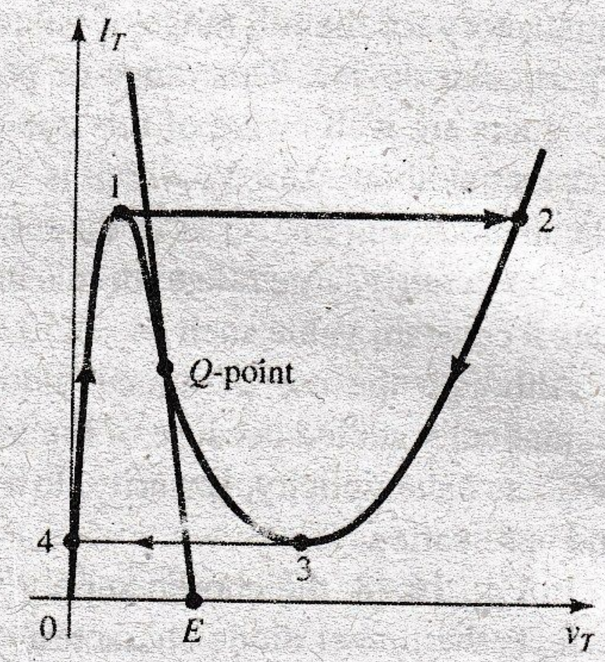

(b)

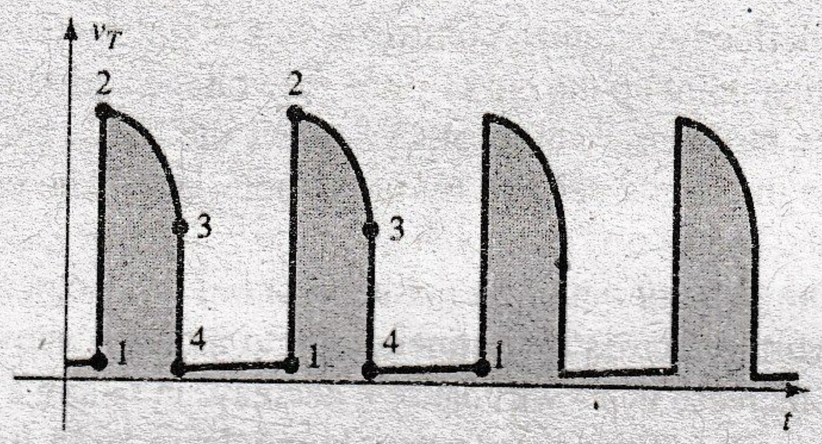

(c)

FIG. 16.49
Negative-resistance oscillator.

characteristics suggest that the current I_T must now decrease with increase in voltage across the diode. This contradicts the fact that

$$E = I_T R + I_T(-R_T)$$

and

$$E = \underbrace{I_T}_{\text{less}}\underbrace{(R - R_T)}_{\text{less}}$$

If both elements of the equation above were to decrease, it would be impossible for the supply voltage to reach its set value. Therefore, for the current I_T to continue rising, the point of operation must shift from point 1 to point 2. However, at point 2, the voltage V_T has jumped to a value greater than the applied voltage (point 2 is to the right of any point on the network load line). To satisfy Kirchhoff's voltage law, the polarity of the transient voltage across the coil must reverse and the current begin to decrease as shown from 2 to 3 on the characteristics. When V_T drops to V_V, the characteristics suggest that the current I_T will begin to increase again. This is unacceptable since V_T is still more than the applied voltage and the coil is discharging through the series circuit. The point of operation must shift to point 4 to permit a continuation of the decrease in I_T. However, once at point 4, the potential levels are such that the tunnel current can again increase from 0 mA to I_P as shown on the characteristics. The process will repeat itself again and again, never settling in on the operating point defined for the unstable region. The resulting voltage across the tunnel diode appears in Fig. 16.49c and will continue as long as the dc supply is energized. The result is an oscillatory output established by a fixed supply and a device with a negative-resistance characteristic. The waveform of Fig. 16.49c has extensive application in timing and computer logic circuitry.

A tunnel diode can also be used to generate a sinusoidal voltage using simply a dc supply and a few passive elements. In Fig. 16.50a, the closing of the switch will result in a sinusoidal voltage that will decease in amplitude with time as shown in Fig. 16.50b. Depending on the elements employed, the time period can be from one almost instantaneous to one measurable in minutes using typical parameter values. This *damping* of the oscillatory output with time is due to the dissipative characteristics of the resistive elements. By placing a tunnel diode in series with the tank circuit as shown in Fig. 16.50c, we can have the negative resistance of the

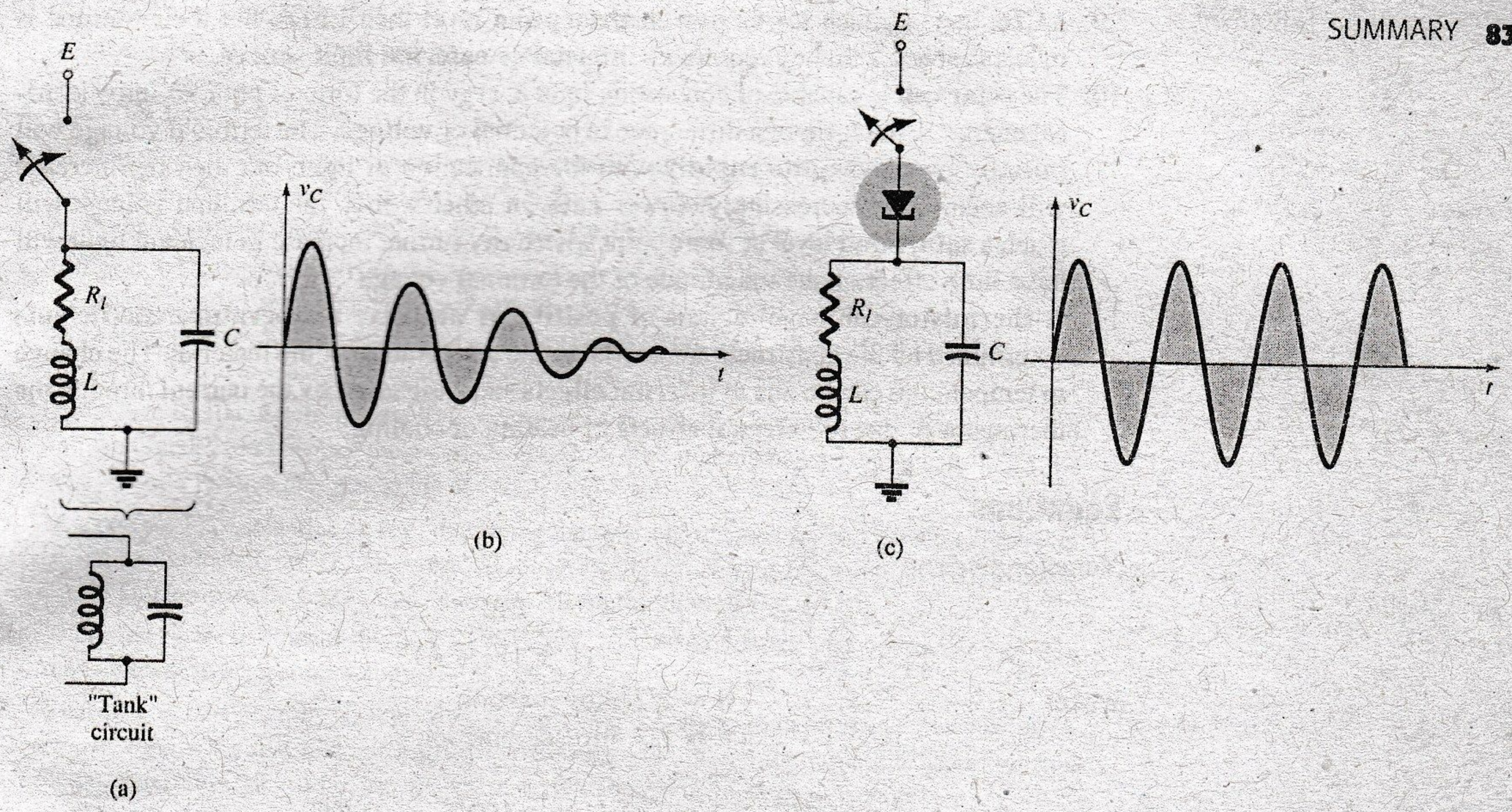

FIG. 16.50
Sinusoidal oscillator.

tunnel diode offset the resistive characteristics of the tank circuit, resulting in the *undamped* response appearing in the same figure. The design must continue to result in a load line that will intersect the characteristics only in the negative-resistance region. In another light, the sinusoidal generator of Fig. 16.50 is simply an extension of the pulse oscillator of Fig. 16.49, with the addition of the capacitor to permit an exchange of energy between the inductor and the capacitor during the various phases of the cycle depicted in Fig. 16.49b.

16.11 SUMMARY

Important Conclusions and Concepts

1. The Schottky barrier (hot-carrier) diode has a **lower threshold voltage** (about 0.2 V), a **larger reverse saturation current**, and a **smaller PIV** than the conventional *p–n* junction variety. It can also be used at higher frequencies because of the reduced reverse recovery time.
2. The varactor (varicap) diode has a **transition capacitance** sensitive to the applied reverse-bias potential that is a maximum at 0 V and that **decreases exponentially** with increasing reverse-bias potentials.
3. The **current capability** of power diodes can be increased by placing two or more in **parallel**, and the **PIV rating** can be increased by stacking the diodes in series.
4. The chassis itself can be used as a **heat sink** for power diodes.
5. **Tunnel diodes** are unique in that they have a **negative-resistance region** at voltage levels less than the typical *p–n* junction threshold voltage. This characteristic is particularly useful in oscillators to establish an oscillating waveform from a switched dc power supply. Due to its reduced depletion region, it is also considered a **high-frequency device** for applications where switching times in nanoseconds or picoseconds are required.
6. The region of operation for **photodiodes** is the **reverse-bias region**. The resulting diode current increases almost **linearly** with an increase in incident light. The **wavelength** of the incident light determines which material will result in the best response; selenium has a good match with the naked eye, and silicon is better for incident light of higher wavelengths.
7. A photoconductive cell is one whose terminal resistance **decreases exponentially** with an **increase in incident light**.
8. An **infrared-emitting diode** emits a beam of radiant flux when **forward-biased**. The strength of the emitted flux pattern is almost **linearly related** to the dc forward current through the device.

9. **LCDs** have a much **lower power absorption level** than LEDs, but their lifetime is much **shorter**, and they require an **internal or external light source**.
10. The **solar cell** is capable of converting light energy in the form of photons into electrical energy in the form of a difference in potential or **voltage**. The terminal voltage will **initially increase quite rapidly** with the application of light, but then the increase will occur at an increasingly **slower rate**. In other words, the terminal voltage will reach a **saturation level** at some point where any further increase in incident light will have little effect on the magnitude of the terminal voltage.
11. A **thermistor** can have regions of **positive or negative temperature coefficients** determined by the construction material or the temperature of the material. The change in temperature can be due to **internal effects** such as caused by the current through the thermistor or due to **external effects** of heating or cooling.

Equations

Varactor diode:

$$C_T(V_R) = \frac{C(0)}{(1 + |V_R/V_T|)^n}$$

where $n = 1/2$ alloy junction
$n = 1/3$ diffused junction

$$TC_C = \frac{\Delta C}{C_0(T_1 - T_0)} \times 100\% \qquad \%/^\circ\text{C}$$

Photodiodes:

$$\lambda = \frac{v}{f} = \frac{3 \times 10^8 \text{ m/s}}{f}$$

$$1\text{Å} = 10^{-10}\text{m} \quad \text{and} \quad 1 \text{ lm} = 1.496 \times 10^{-10} \text{ W}$$

$$1 \text{ fc} = 1 \text{ lm/ft}^2 = 1.609 \times 10^{-9} \text{ W/m}^2$$

Solar cells:

$$\eta = \frac{P_{o(\text{electrical})}}{P_{i(\text{light energy})}} \times 100\%$$

$$= \frac{P_{\max(\text{device})}}{(\text{area in cm}^2)(100 \text{ mW/cm}^2)} \times 100\%$$

PROBLEMS

**Note:* Asterisks indicate more difficult problems.

16.2 Schottky Barrier (Hot-Carrier) Diodes

1. **a.** Describe in your own words how the construction of the hot-carrier diode is significantly different from the conventional semiconductor diode.
   b. In addition, describe its mode of operation.
2. **a.** Consult Fig. 16.2. Compare the dynamic resistances of the diodes in the forward-bias regions.
   b. How do the levels of I_s and V_Z compare?
3. Using the data of Fig. 16.5, determine the reverse leakage current at a temperature of 50°C. Assume a linear relationship between the two quantities.
4. (a) Using the electrical characteristics of Fig. 16.5, find the reactance of the capacitor at a frequency of 1 MHz and a reverse voltage of 1 V. (b) Find the forward dc resistance of the diode at 10 mA.
5. **a.** Using the data from Fig. 16.5 plot the forward current versus forward voltage for the Schottky diode.
   b. Determine the piecewise equivalent resistance for the vertical rise section of the characteristics.
   c. What is the resulting vertical break voltage for the diode as compared to the 0.7 V value typically used for a *p–n* junction diode.
6. Using the plot of Fig. 16.6a,
   a. What is the forward voltage at a current of 50 mA (note the log scale) at room temperature (25°C).
   b. What is the forward voltage at the same current as part (a) but a temperature of 125°C?
   c. What can be said about the effect of temperature on the resulting voltage drop across a Schottky diode as the temperature increases?

7. Using the characteristics of Fig. 16.6(c), determine the reactance of the diode capacitor at a frequency of 1 MHz and a reverse bias potential of 1 V. Is it significant?

16.3 Varactor (Varicap) Diodes

8. **a.** Determine the transition capacitance of a diffused junction varicap diode at a reverse potential of 4.2 V if $C(0) = 80$ pF and $V_r = 0.7$ V.
   b. From the information of part (a), determine the constant K in Eq. (16.2).
9. **a.** For a varicap diode having the characteristics of Fig. 16.7, determine the difference in capacitance between reverse-bias potentials of -3 V and -12 V.
   b. Determine the incremental rate of change ($\Delta C/\Delta V_r$) at $V = -8$ V. How does this value compare with the incremental change determined at -2 V?
*10. Using Fig. 16.10a, determine the total capacitance at a reverse potential of 1 V and 8 V and find the tuning ratio between these two levels. How does it compare to the tuning ratio for the ratio between reverse bias potentials of 1.25 V and 7 V?
11. At a reverse-bias potential of 4 V, determine the total capacitance for the varactor from Fig. 16.10a and calculate the Q value from $Q = 1/(2\pi f R_S C_t)$ using a frequency of 10 MHz and $R_s = 3\ \Omega$. Compare to the Q value determined from the chart of Fig. 16.10a.
12. Determine T_1 for a varactor diode if $C_0 = 22$ pF, $TC_C = 0.02\%/°C$, and $\Delta C = 0.11$ pF due to an increase in temperature above $T_0 = 25°C$.
13. What region of V_R would appear to have the greatest change in capacitance per change in reverse voltage for the diode of Fig. 16.10? Be aware that it is a log-log scale. Then, for this region, determine the ratio of the change in capacitance to the change in voltage.
*14. Using Fig. 16.10a, compare the Q levels at a reverse bias potential of 1 V and 10 V. What is the ratio between the two? If the resonant frequency is 10 MHz, what is the bandwidth for each bias voltage? Compare the bandwidths obtained and compare their ratio to the ratio of Q levels.
15. Referring to Fig. 16.11, if $V_{DD} = 2$ V for the varactor of Fig. 16.10, find the resonant frequency of the tank circuit if $C_C = 40$ pF and $L_T = 2$ mH.

16.4 Solar Cells

16. A 1-cm by 2-cm solar cell has a conversion efficiency of 9%. Determine the maximum power rating of the device.
*17. If the power rating of a solar cell is determined on a very rough scale by the product $V_{OC}\, I_{SC}$, is the greatest rate of increase obtained at lower or higher levels of illumination? Explain your reasoning.
18. **a.** For the solar cell of Fig. 16.13, determine the ratio $\Delta I_{SC}/\Delta fc$ if $fc_1 = 20fc$.
    b. Using the results of part (a), find the level of I_{SC} resulting from a light intensity of 28 footcandles.
19. **a.** For the solar cell of Fig. 16.14, determine the ratio $\Delta IV_{OC}/\Delta fc$ for the range of 20 fc to 100 fc if $fc_1 = 40fc$.
    b. Using the results of part (a), determine the expected level of V_{OC} at a light intensity of 60 fc.
20. **a.** Plot the 1-V curve for the same solar cell of Fig. 16.15 but with a light intensity of fc_1.
    b. Plot the resulting power curve from the results of part (a).
    c. What is the maximum power rating? How dews it compare to the maximum power rating for a light intensity fc_2?
21. **a.** What is the energy in joules associated with photons that have a wavelength matching that of the color blue in the visible spectrum?
    b. Repeat part (a) for the color red.
    c. Do the results confirm the fact that the shorter the wavelength the higher the energy level?
    d. Is light in the ultraviolet range more dangerous in regard to skin cancer than those in the infrared range? Why?
    e. Can you guess why fluorescent lights are used for growing plants in a dark environment?

16.5 Photodiodes

22. Referring to Fig. 16.20, determine I_λ if $V_\lambda = 30$ V and the light intensity is 4×10^{-9} W/m^2.
*23. Determine the voltage drop across the resistor of Fig. 16.19 if the incident flux is 3000 fc, $V_\lambda = 25$ V, and $R = 100$ kΩ. Use the characteristics of Fig. 16.20.
24. Write an equation for the diode current of Fig. 16.22 versus the applied light intensity in footcandles.

16.6 Photoconductive Cells

*25. What is the approximate rate of change of resistance with illumination for a photoconductive cell with the characteristics of Fig. 16.26 for the ranges (a) 0.1 → 1 kΩ, (b) 1 → 10 kΩ, and (c) 10 → kΩ? (Note that this is a log scale.) Which region has the greatest rate of change in resistance with illumination?

26. What is the "dark current" of a photodiode?

27. If the illumination on the photoconductive diode in Fig. 16.28 is 10 fc, determine the magnitude of V_i to establish 6 V across the cell if R_1 is equal to 5 kΩ. Use the characteristics of Fig. 16.26.

*28. Using the data provided in Fig. 16.27, sketch a curve of percentage conductance versus temperature for 0.01, 1.0, and 100 fc. Are there any noticeable effects?

*29. a. Sketch a curve of rise time versus illumination using the data from Fig. 16.27.
b. Repeat part (a) for the decay time.
c. Discuss any noticeable effects of illumination in parts (a) and (b).

30. Which colors is the CdS unit of Fig. 16.27 most sensitive to?

16.7 IR Emitters

31. a. Determine the radiant flux at a dc forward current of 70 mA for the device of Fig. 16.30.
b. Determine the radiant flux in lumens at a dc forward current of 45 mA.

*32. a. Through the use of Fig. 16.31, determine the relative radiant intensity at an angle of 25° for a package with a flat glass window.
b. Plot a curve of relative radiant intensity versus degrees for the flat package.

*33. If 60 mA of dc forward current is applied to an SG1010A IR emitter, what will be the incident radiant flux in lumens 5° off the center if the package has an internal collimating system? Refer to Figs. 16.30 and 16.31.

16.8 Liquid-Crystal Displays

34. Referring to Fig. 16.35, which terminals must be energized to display number 7?

35. In your own words, describe the basic operation of an LCD.

36. Discuss the relative differences in mode of operation between an LED and an LCD display.

37. What are the relative advantages and disadvantages of an LCD display as compared to an LED display?

16.9 Thermistors

*38. For the thermistor of Fig. 16.40, determine the dynamic rate of change in specific resistance with temperature at $T = 20°C$. How does this compare to the value determined at $T = 300°C$? From the results, determine whether the greatest change in resistance per unit change in temperature occurs at lower or higher levels of temperature. Note the vertical log scale.

39. Using the information provided in Fig. 16.40, determine the total resistance of a 2-cm length of the material having a perpendicular surface area of 1 cm^2 at a temperature of 0°C. Note the vertical log scale.

40. a. Referring to Fig. 16.41, determine the current at which a 25°C sample of the material changes from a positive to a negative temperature coefficient. (Figure 16.41 is a log scale.)
b. Determine the power and resistance levels of the device (Fig. 16.41) at the peak of the 0°C curve.
c. At a temperature of 25°C, determine the power rating if the resistance level is 1 MΩ.

41. In Fig. 16.43, $V = 0.2$ V and $R_{variable} = 10\ \Omega$. If the current through the sensitive movement is 2 mA and the voltage drop across the movement is 0 V, what is the resistance of the thermistor?

16.10 Tunnel Diodes

42. What are the essential differences between a semiconductor junction diode and a tunnel diode?

*43. Note in the equivalent circuit of Fig. 16.45 that the capacitor appears in parallel with the negative resistance. Determine the reactance of the capacitor at 1 MHz and 100 MHz if $C = 5$ pF, and determine the total impedance of the parallel combination (with $R = -152\ \Omega$) at each frequency. Is the magnitude of the inductive reactance anything to be overly concerned about at either of these frequencies if $L_S = 6$ nH?

*44. Why do you believe the maximum reverse current rating for the tunnel diode can be greater than the forward current rating? (*Hint:* Note the characteristics and consider the power rating.)

45. Determine the negative resistance for the tunnel diode of Fig. 16.44 between $V_T = 0.1$ V and $V_T = 0.3$ V.

46. Determine the stable operating points for the network of Fig. 16.48 if $E = 2$ V, $R = 0.39$ kΩ, and the tunnel diode of Fig. 16.44 is employed.

*47. For $E = 0.5$ V and $R = 51\ \Omega$, sketch v_T for the network of Fig. 16.49 and the tunnel diode of Fig. 16.44.

48. Determine the frequency of oscillation for the network of Fig. 16.50 if $L = 5$ mH, $R_l = 10\ \Omega$, and $C = 1\ \mu F$.